Zeitschrift: Schweizerische mineralogische und petrographische Mitteilungen = Bulletin suisse de minéralogie et pétrographie

Band: 80 (2000)

Heft: 3

Artikel: Tourmaline-rich ore-bearing hydrothermal system of lower Valle del Cervo (western Alps, Italy) : field relationships and petrology

Autor: Bernardelli, Paola / Castelli, Daniele / Rossetti, Piergiorgio

DOI: https://doi.org/10.5169/seals-60965

SCHWEIZ. MINERAL. PETROGR. MITT. 80, 257–277, 2000

Tourmaline-rich ore-bearing hydrothermal system of lower Valle del Cervo (western Alps, Italy): field relationships and petrology

by *Paola Bernardelli*[1], *Daniele Castelli*[1] and *Piergiorgio Rossetti*[1]

Abstract

A late-Alpine tourmaline-rich (up to 90%), ore-bearing hydrothermal system crops out in the Sesia Zone (and its andesite cover) in the roof portion of the Oligocene Valle del Cervo (VDC) Pluton. This system consists of multistage hydrothermal veins and breccia pipes, showing a variety of mineral assemblages and textures that are novel in the western Alps. An early depositional episode consisting of scanty K-feldspar ± tourmaline veins was followed by the main three-stage episode which consists of ore-bearing tourmaline, tourmaline + quartz and quartz + carbonate veins, and breccia pipes. A final subordinate episode consists mainly of ore-poor carbonate + quartz veins. Tourmalines is commonly zoned and occurs in various microstructural settings, with associated changes in composition that cover a range within the dravite-schorl-povondraite-uvite series. The most abundant ore minerals are sulfides (pyrite, chalcopyrite, arsenopyrite, tetrahedrite, galena and Bi-sulphosalts) and minor scheelite plus magnetite. Wallrock alteration differs in both intensity and mineral assemblages according to vein types and host rock.

The deeper part of the system (closer to VDC Pluton) is characterized by both veins and breccia pipes and is strongly enriched in tourmaline. In the upper part of the system, breccia pipes do not occur and hydrothermal veins are strongly enriched in ore minerals (including hessyte, tetradymite and Bi-sulphosalts). Occurrence of hydrothermal breccia structures and abundant tourmaline correlate the hydrothermal system to the evolution of late-magmatic, boron-rich fluids, exsolved from the shallow-level solidifying VDC intrusion. Preliminary estimates based on geologic and petrologic data suggest that the lower part of the system developed at a maximum depth of about 2 km and at $T \leq 450$ °C.

Keywords: tourmaline, ore minerals, hydrothermal activity, Oligocene magmatism, western Alps, Sesia Zone.

1. Introduction

Tourmaline is a common accessory phase in a variety of sedimentary, igneous and metamorphic rocks. It has also long been recognized as an important gangue mineral in metallic and non-metallic ore deposits. Particularly, tourmaline is commonly an important phase in many types of hydrothermal ore deposits (SLACK, 1996, and references therein). In hydrothermal systems, tourmaline-rich rocks are often associated with Cu and/or Mo ± Au ores related to I-type granitic rocks and comagmatic volcanics (SILLITOE and SAWKINS, 1971; WARNAARS, 1983; SILLITOE, 1985; WARNAARS et al., 1985; SLACK, 1996; LYNCH and ORTEGA, 1997). Alternatively, tourmaline-rich rocks can be associated with Sn–W ores related to peraluminous S-type granite (ALLMAN-WARD et al., 1982; JACKSON et al., 1982, 1989; LONDON and MANNING, 1995; LONDON et al., 1996; SLACK, 1996). In submarine-hydrothermal systems, stratabound tourmaline-rich rocks are typically linked to Pb–Zn ores (KNOPF, 1913; SLACK, 1996, and references therein).

In the past, rocks containing in excess of 15–20% tourmaline have been named tourmalinites, regardless of their geometry and origin (ALLMAN-WARD et al., 1982; CHAROY, 1982). However, the term tourmalinite has been recently used for stratabound tourmaline-rich rocks only (SLACK, 1996), and it will not be used hereafter.

In the internal western Alps, tourmaline-rich (up to 90%) rocks occur in the Sesia Zone of lower Valle del Cervo (VDC), close to the late-Alpine

[1] Dipartimento di Scienze Mineralogiche e Petrologiche, Università di Torino, Via Valperga Caluso 35, I-10125 Torino, Italy. <castelli@dsmp.unito.it> and <rossetti@dsmp.unito.it>

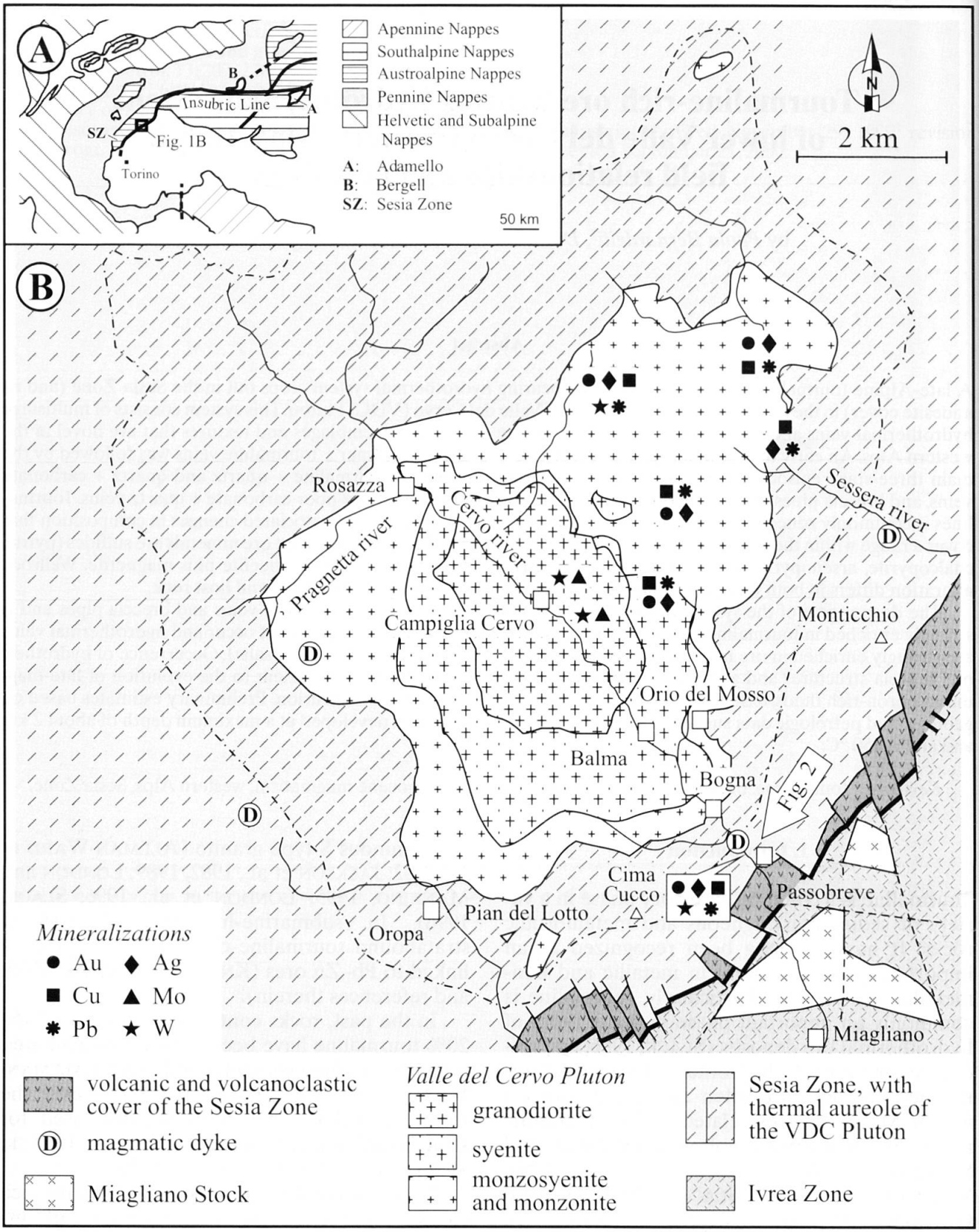

Fig. 1 Geological sketch map of the VDC area (compiled after FIORENTINI POTENZA, 1959; CARRARO and FERRARA, 1968; FORNASERO, 1978; VENTURELLI et al., 1984; BIGI et al., 1990; AQUATER, 1994; MEDEOT, 1998; TREVISIOL, 1999). IL: Insubric Line. Lithological subdivisions of the VDC Pluton (based on FIORENTINI POTENZA, 1959) broadly correspond to Granite, Syenite and Monzonite Complexes of BIGIOGGERO et al. (1994).

VDC Pluton. The literature on these rocks is very limited. CARRARO (1962) interpreted them as mylonites rich in tourmaline and pyrite. By contrast, in several unpublished mining reports (RIMIN, 1989; AQUATER, 1992, 1994), they were regarded as hydrothermal rocks, but the available descriptions are brief. Our field and analytical work shows that they are polymetallic, sulfide- and tourmaline-rich hydrothermal veins and breccia pipes, likely related to Oligocene magmatism.

In this paper we describe, for the first time, the occurrence and evolution of a late-Alpine ore-bearing boron-rich hydrothermal system in the Alps. Detailed geologic, petrographic and analytical data are given, and a multistage evolution of the hydrothermal system is described. Relationships with the VDC Oligocene magmatism are also discussed and compared to other ore-bearing, boron-rich magmatic-hydrothermal systems from the literature.

2. Geologic setting

The Oligocene magmatism in the VDC area consists of plutons, volcanic to volcanoclastic sequences and minor dykes (Fig. 1). The VDC Pluton is a composite stock (FIORENTINI POTENZA, 1959) that intruded eclogite-facies rocks (metapelite, orthogneiss and eclogite) of the Austroalpine Sesia Zone (COMPAGNONI et al., 1977; FORNASERO, 1978; DROOP et al., 1990) at 30–31 Ma (Rb/Sr biotite age: BIGIOGGERO et al., 1994; U/Pb zircon age: ROMER et al., 1996). FIORENTINI POTENZA (1959) first described a concentric arrangement within this stock, with a granitic core rimmed by syenitic to monzonitic coronas. BIGIOGGERO et al. (1994) introduced a subdivision in "complexes": the Granitic, Syenitic and Monzonitic Complex, respectively. The three Complexes belong to a same shoshonitic series, with high contents of LILE and HFSE (BIGIOGGERO et al., 1994). TREVISIOL (1999) recently classified rocks of the Granitic Complex as quartz-poor granodiorite. The smaller Miagliano Stock, emplaced in the Southalpine Ivrea Zone, shows dioritic–monzonitic composition (CARRARO and FERRARA, 1968). Radiometric Rb/Sr and K/Ar biotite ages from this intrusive, reported as 31 Ma (CARRARO and FERRARA, 1968), have been recalculated to model ages of 31–34 Ma by BIGIOGGERO et al. (1994).

The volcanic to volcanoclastic sequences occur as a narrow belt between the Sesia and the Ivrea Zones, northwest of the Insubric Line (Fig. 1). They consist of lava flows, pyroclastic and epiclastic deposits (locally with fragments of basement rocks of the Sesia Zone: BIANCHI and DAL PIAZ, 1963). Compositions range from basaltic andesite and andesite of high-K calc-alkaline affinity to trachyandesite and trachydacite of shoshonitic affinity (MEDEOT et al., 1997; MEDEOT, 1998). Contrary to earlier views that included these rocks in the Canavese Zone (see COMPAGNONI et al., 1977, for a discussion), they have been dated at 29–33 Ma and are now interpreted as part of the Tertiary post-metamorphic cover of the Sesia Zone (HUNZIKER, 1974; SCHEURING et al., 1974; ZINGG et al., 1976; COMPAGNONI et al., 1977; BIINO and COMPAGNONI, 1989). Based on their common geochemical characteristics, these volcanic rocks and the VDC Pluton have been recently interpreted as part of a single volcano-plutonic complex (MEDEOT et al., 1997).

A variety of magmatic dykes, showing high-K calc-alkaline to shoshonitic affinity (BECCALUVA et al., 1983; VENTURELLI et al., 1984), was emplaced at about 32 Ma (Rb/Sr biotite age, BIGIOGGERO et al., 1983) in both the Sesia and Ivrea Zones. The occurrence of a magmatic dyke (Fig. 1) has also been reported within the monzonitic rim of the VDC Pluton (BIGI et al., 1990).

Palaeomagnetic data on magmatic dykes and andesitic cover of the Sesia Zone (LANZA, 1977, 1979) and on the southernmost Traversella Oligocene Pluton (LANZA, 1984) suggest that the internal Sesia Zone and the Oligocene magmatics underwent a clockwise rotation around a NE-striking subhorizontal axis. This tilting (60–70° according to LANZA, 1977, 1979; and 40–50° according to LANZA, 1984) is in agreement with the current attitude of volcanic cover (strongly dipping towards SE) of the Sesia Zone. Therefore: (i) in the VDC area an upper crustal section from deeper (at NW) to shallower (at SE) levels is exposed, respectively, and (ii) the Sesia rocks occurring between the pluton and the Insubric Line broadly represent the roof of the VDC Pluton (Fig. 1).

A variety of hydrothermal features are linked to the intrusion of VDC Pluton (RIMIN, 1989; AQUATER, 1992, 1994). Within the intrusion, they mainly occur in the central to northeastern part of the body. Particularly, thin Mo and W-bearing quartz veins occur in the granodioritic core, whereas Cu, Pb, Ag, Au and minor W-bearing quartz veins occur in both the syenitic and monzonitic rims (Fig. 1). In both the Sesia Zone country-rocks and the volcano-sedimentary cover, hydrothermal features include Cu, Pb, W, Au and Ag-bearing veins. Hydrothermal veins within the Sesia rocks only occur southeast of the VDC Pluton (in both Cervo and northernmost Sessera valleys) and often consist of tourmaline-rich veins and breccia bodies. In this paper, we focus on

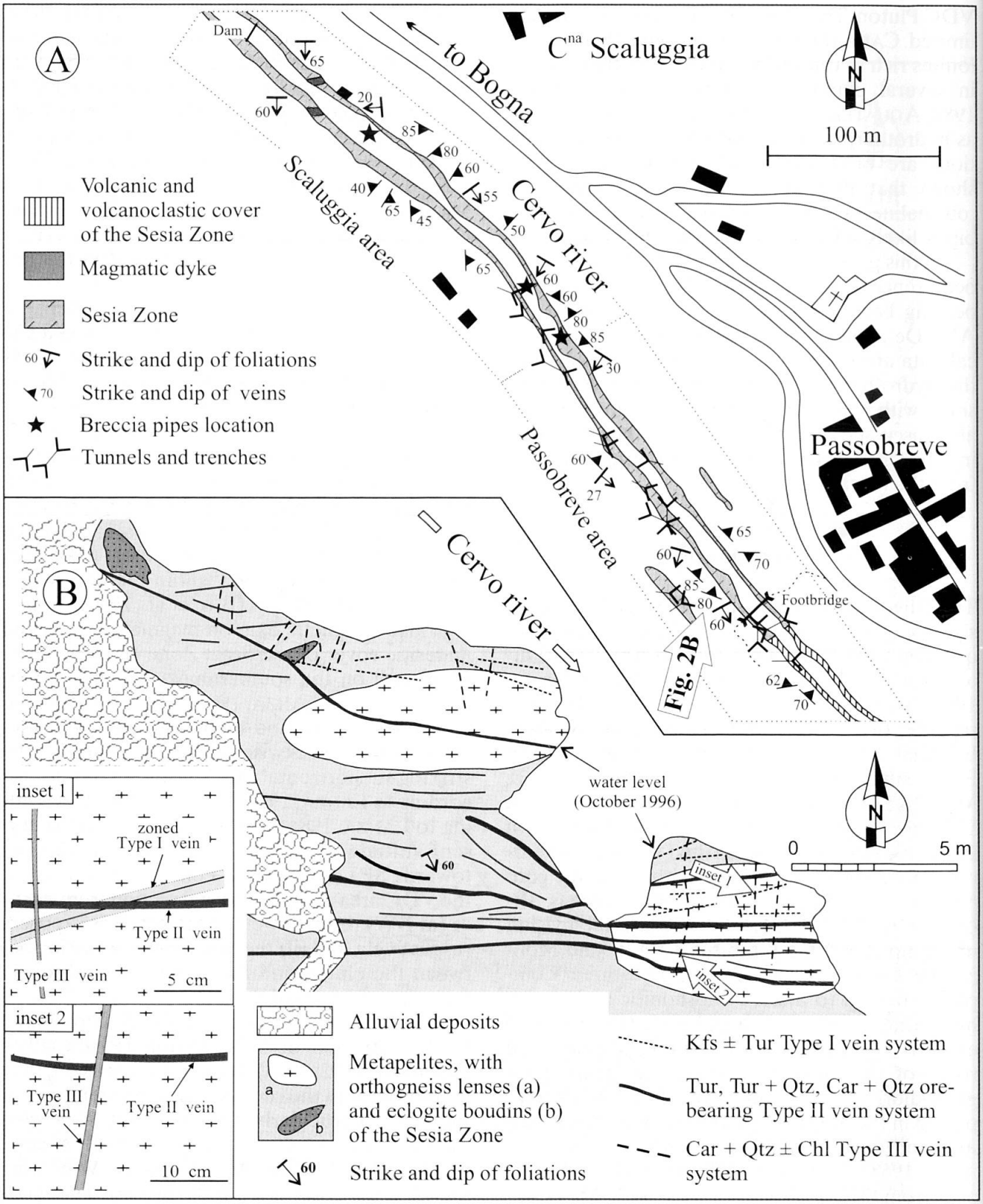

Fig. 2 (A) Simplified geological map of VDC southeast of Bogna, showing the location of hydrothermal tourmaline-rich vein systems and breccia pipes within the Sesia Zone and Oligocene volcanics (modified after BERNARDELLI, 1998). Passobreve and Scaluggia areas outlined by dotted lines are discussed in text. Orientations mainly refer to Type II vein system.
(B) Detailed geological sketch of hydrothermal vein systems within the Sesia Zone along the right bank of Cervo river, in the southern Passobreve area (modified after BERNARDELLI, 1998). Location of footbridge across river (Fig. 2A) is about 10 m SE of area shown. Mesostructural relationships between Type I to Type III vein systems are shown in two insets. Mineral abbreviations according to table 1.

polymetallic, sulfide- and tourmaline-rich rocks cropping out in both the Sesia Zone and its volcanic cover, along the lower VDC (Fig. 1).

3. Field relations and petrography

Along the Cervo river southeast of Bogna, the Sesia rocks consist of metapelite schist with orthogneiss lenses and minor metabasite boudins (Figs 1 and 2). The contact between Sesia Zone and andesite volcanics occurs near the footbridge southwest of Passobreve. Magmatic dykes in the Sesia metapelite, strongly altered by carbonate-quartz hydrothermal veinlets, crop out west-southwest of Scaluggia.

The tourmaline-rich ore-bearing hydrothermal system crops out along both banks of the Cervo river (Passobreve and Scaluggia areas in Fig. 2A) and crosscuts all different rock types. It starts about 400 m southeast of the intrusive contact and extends into the Oligocene andesite volcanics. The hydrothermal system consists of veins and breccia pipes which used to be exploited for copper, mostly during the 19th century (AQUATER, 1994), as testified by the presence of small trenches and tunnels (Fig. 2A).

Based on fieldwork and petrography, three different vein systems (hereafter called Type I to III vein systems) have been recognized, showing variable attitude, thickness and composition. Field relationships are well exposed along the Cervo river, and are shown in the geological sketch map of a selected outcrop at Passobreve (Fig. 2B). As shown in Fig. 2B, crosscutting relationships allow to arrange Type I to Type III vein systems from older to younger, respectively. The breccia pipes are ascribed to the Type II vein system and will be discussed below. A summary of time relationships and paragenetic sequences of vein minerals is given in Fig. 3. Mineral symbols according to KRETZ (1983) and other mineral abbreviations used hereafter are given in table 1.

3.1. TYPE I VEIN SYSTEM

The Type I vein system only crops out within the Sesia rocks of the Passobreve area (Fig. 2), and is represented by subvertical veins striking N75° to 110°. These are whitish veins, up to 1.5 cm thick and few metres long, mainly consisting of K-feldspar ± tourmaline.

The thinner veins are homogeneous and consist of fine-grained K-feldspar (70%), with minor chlorite, carbonate (mostly ankerite: $CaMg_{0.4}Fe_{0.5}Mn_{0.1}[CO_3]_2$), quartz and accessory titanite, pyrite and chalcopyrite. K-feldspar is Ba-enriched ($Or_{91-93}Ab_{5-7}Cs_{1-4}$) and occurs both as aggregates of xenomorphic to subidiomorphic grains, and as isolated idiomorphic crystals with rhombohedral shape (adularia?). It also shows a slight increase of barium contents from core to rim. Chlorite (ripidolite–brunsvigite) commonly develops at vein walls.

The thickest veins are symmetrically zoned with an external whitish portion and an inner black portion (Fig. 4A). The external part shows the same fabric and mineralogy as the thinner veins, whilst the inner portion consists of tourmaline and very minor carbonate, quartz and chalcopyrite. Under the microscope, the tourmaline-rich portion often shows a brecciated structure, consisting of a very fine-grained tourmaline matrix including small fragments of the external portion (Figs 3 and 4A).

3.2. TYPE II VEIN SYSTEM

Type II is the most important vein system and consists of tourmaline, quartz, carbonate and sulfides as black to reddish veins occurring in both the Sesia and volcanic rocks. In the Passobreve area, the veins are subvertical and mostly strike N80–N110°. Approaching the contact with the VDC Pluton (Scaluggia area), the same vein system strikes N20–N50°, dipping northwest 40–50° and southeast 45–80° (Fig. 2). Veins are millimetre to decimetre thick, and up to tens of metres long. The thickest veins (~50 cm) developed close to the contact with the VDC stock, while the thinner ones occur within the volcano-sedimentary sequence.

Meso- to microstructural relationships and mineral assemblages indicate different domains within a single vein and suggest a multistage evolution of Type II vein system (Fig. 3). Types IIa and IIb domains have been observed only within the Sesia rocks, whilst Type IIc domains occur in both the Sesia (particularly at Passobreve) and volcanic rocks.

Type IIa domains

Type IIa domains consist of tourmaline and very minor quartz, sulfides and titanite (Fig. 4B). Tourmaline occurs as brecciated aggregates, cemented by a finer grained tourmaline matrix. The tourmaline "clasts" are more abundant and coarser grained (up to few millimetres) approaching the intrusion (Scaluggia area in figure 2). Tourmaline (up to 90%) always occurs as euhedral crystals, ranging from olive green to brownish in colour under the microscope. Both within the clasts

and in the matrix, it shows a discontinuous zoning, with deeper coloured rims. Quartz and titanite, as well as euhedral pyrite and anhedral chalcopyrite, occur in both clasts and fine grained matrix.

Type IIb domains

These are the most important, ore-bearing domains of Type II vein system and consist of variable amount of fine grained tourmaline (10–70%), quartz (15–60%) and ore minerals, with minor chlorite and accessory K-feldspar, apatite and titanite. Type IIb domains crosscut or contain brecciated Type IIa domains up to few centimetres in size (Fig. 4C).

Type IIb tourmaline is also olive green to brownish in colour, but shows less zoning than tourmaline in Type IIa domains. Tourmaline crystals are typically fine-grained, prismatic to acicular in shape, and grow perpendicular to the surface of Type IIa clasts. Quartz is fine-grained, anhedral to subhedral in shape, and often includes tourmaline. Chlorite (ripidolite-pycnochlorite) has only been observed in veins crosscutting Sesia metabasites. Ba-enriched K-feldspar ($Or_{94-95}Ab_{3-5}Cs_{0.7-1.9}$) occasionally occurs, as fine-grained anhedral grains often showing a cloudy appearance. Some ankeritic carbonate may also occur in the Scaluggia area.

Ore minerals (idiomorphic pyrite armoured by anhedral chalcopyrite, minor tetrahedrite, scheelite and arsenopyrite) are commonly arranged as centimetre-thick pods, but also occur as either disseminated grains or small stockworks. Silver-rich tetrahedrite forms irregular patches cementing the gangue minerals. Scheelite occurs as fractured idiomorphic crystals, whose fractures are filled by pyrite and chalcopyrite. Arsenopyrite occurs as either disseminated idiomorphic grains or anhedral inclusions in pyrite. Very fine-grained thorite and sphalerite are locally present. Where Type IIb domains crosscut the Sesia metabasites, the only ore minerals are magnetite and minor pyrite.

Type IIc domains

Type IIc are medium-grained, tourmaline-free domains consisting of quartz and carbonate, with minor chlorite, albite and titanite. Major ore minerals are chalcopyrite, pyrite, galena, tetrahedrite,

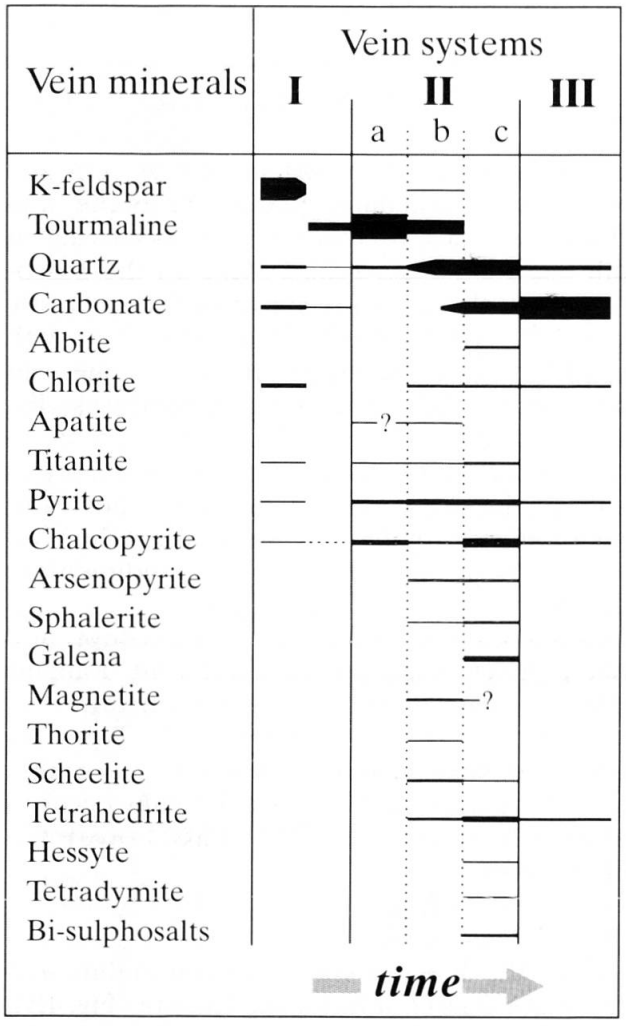

Fig. 3 Summary of temporal relations among hydrothermal mineral assemblages in different vein systems from the Passobreve and Scaluggia areas. The bar thickness relates to estimated mineral proportions during each stage (each set to 100%). Note that mineral assemblages in Type II veins are arranged according to different domains (IIa to IIc), from earlier to later (see text for discussion). Mineral abbreviations according to table 1.

Tab. 1 Mineral abbreviations.

Ab	Albite	Jd	Jadeite
Amp	Ca-amphibole	Kfs	K-feldspar
And	Andalustie	Ky	Kyanite
Ap	Apatite	Mag	Magnetite
Apy	Arsenopyrite	Ms	Muscovite
Bi-Spt	Bi-sulphosalts	Ol	Olivine
Bt	Biotite	Omp	Omphacite
Car	Carbonate	Opx	Orthopyroxene
Ccp	Chalcopyrite	Ph	Phengite
Chl	Chlorite	Pl	Plagioclase
Cpx	Clinopyroxene	Py	Pyrite
Crd	Cordierite	Qtz	Quartz
Crn	Corundum	Rt	Rutile
Ep	Epidote	Sch	Scheelite
FeCrd	Fe-Cordierite	Ser	Sericite
Gln	Glaucophane	Sil	Sillimanite
Gn	Galena	Sp	Sphalerite
Gr	Graphite	Ter	Tetrahedrite
Grt	Garnet	Tho	Thorite
Hes	Hessyte	Tm	Tetradymite
Hbl	Hornblende	Ttn	Titanite
Ilm	Ilmenite	Tur	Tourmaline

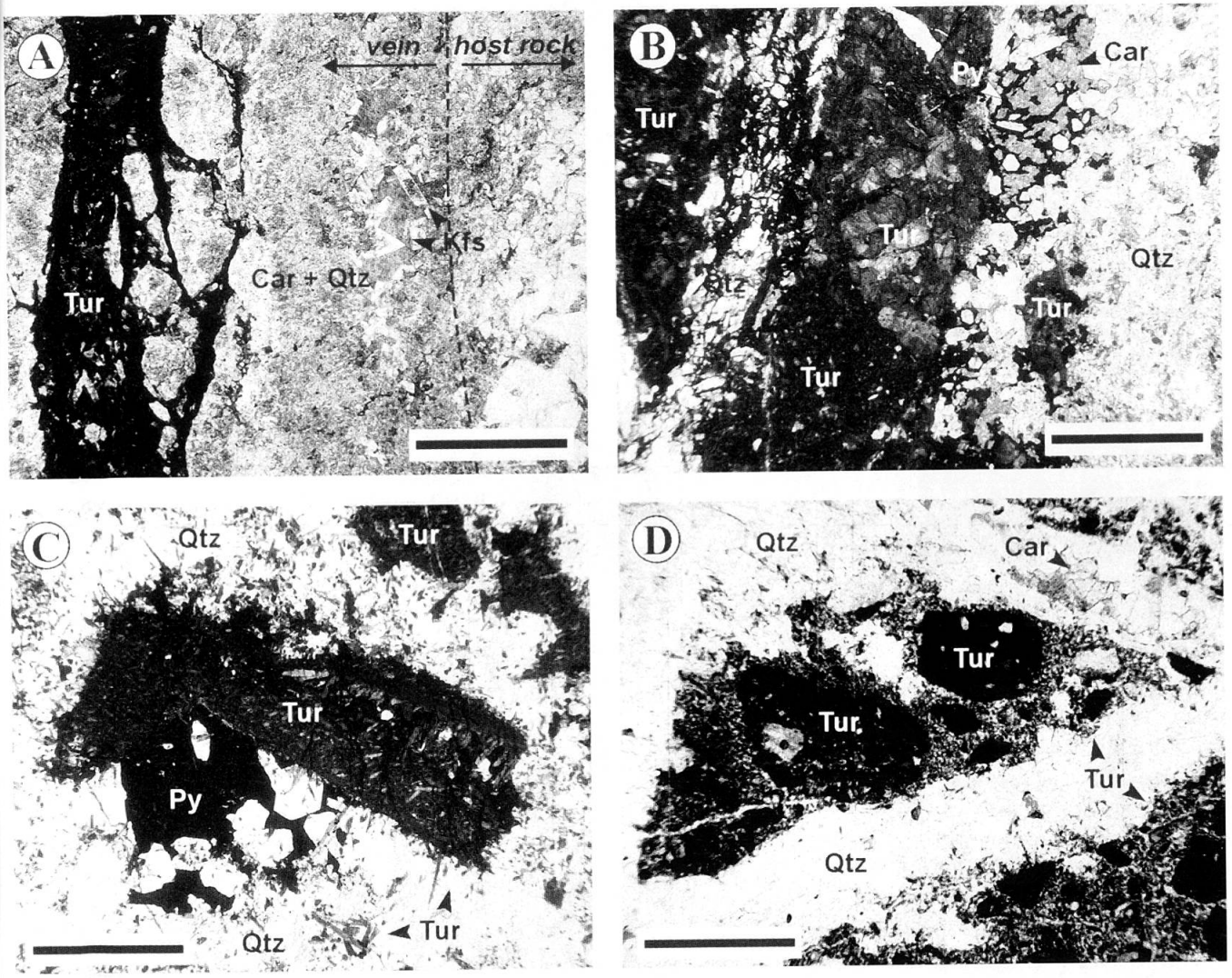

Fig. 4 Selected occurrences of tourmaline in different vein systems. Plane polarized light, 1 mm scale bar; mineral abbreviations as in table 1. (A) *K-feldspar ± tourmaline Type I vein.* Microphotograph shows half of a symmetrically zoned vein, whose inner part consists of fine-grained tourmaline. The outer vein portion mainly consists of idioblastic K-feldspar within fine-grained carbonate + quartz aggregates. Towards the centre of vein the Car + Qtz matrix is brecciated and armoured by very fine-grained tourmaline. To the right, the Sesia orthogneiss host is altered to K-feldspar, fine-grained chlorite intergrown with minor carbonate. Sample TV297, Passobreve area. (B) *Microstructural relationships in multistage Type II vein.* Tourmaline-rich Type IIa domains (with irregular shape, at centre and to the left) are armoured by Qtz + Car + Py Type IIc domains. Within the clastic Type IIa domains, tourmaline occurs as both large zoned crystals and finer grained Tur ± Qtz aggregates. In Type IIc domains quartz is mostly idiomorphic and pyrite is interstitial to rounded carbonate grains. Sample TV319, Scaluggia area. (C) *Microstructural relationships in multistage Type II vein.* Clasts of tourmaline-rich Type IIa domains are set in a matrix composed of quartz, very fine-grained tourmaline and interstitial pyrite (Type IIb domain). Fine grained tourmaline typically grows perpendicularly to Type IIa clasts. Sample TV304, Passobreve area. (D) *Microstructural relationships between different domains in breccia pipe.* Tourmaline-rich composite clasts (at centre and bottom right) are surrounded by quartz + carbonate Type IIc-like domain. Within the clasts, two different domains consist of clasts of tourmaline aggregates (Type IIa-like domains, darker areas) embedded in fine grained tourmaline + quartz matrix (Type IIb-like domains). Sample TV318, Scaluggia area.

scheelite, Bi-sulphosalts and sphalerite. The relative abundance of minerals is highly variable. Carbonate (ankerite: $CaMg_{0.4-0.5}Fe_{0.3-0.4}Mn_{0.1-0.2}[CO_3]_2$) ranges from 10 to 50%, quartz from 15 to 70%, and ore minerals from near zero to 40%. Type IIc domains again crosscut or contain brecciated Type IIa and IIb domains (Fig. 4B).

The fabric of Type IIc domains depends on the host rock. In veins across Sesia metapelite and orthogneiss, euhedral quartz develops perpendicular to the vein walls (comb texture) and/or to Type IIa and IIb clasts (cockade-like texture), whilst carbonate occurs in the inner part. In the volcanics, anhedral quartz and chlorite (ripidolite–

Tab. 2 Alteration assemblages related to Type I, II and III vein systems in different lithologies.

Host rock	Primary assemblages[1)]	Alteration assemblages[2)]		
		Type I	**Type II**	**Type III**
metapelite	Qtz + Ph + Grt ± Omp, Rt, Gr	Kfs + Chl + Car ± Bt, Ttn, Ilm, Py	Qtz + Ser + Car ± Kfs, Ab, Tur, Py, Gr	Car + Ser ± Chl, Ttn, Py
orthogneiss	Jd + Qtz + Ph ± Kfs, Rt			
metabasite	Grt + Omp + Gln + Rt ± Ph	Bt + Chl + Amp + Ep + Kfs + Ab + Car + Py + Mag ± Ilm	Chl + Car ± Kfs, Ab, Qtz, Tur, Ilm, Ttn, Py	—
andesite *s.l.*	Pl + Hbl + Cpx ± Opx, Bt, Ol		Car + Qtz + Chl ± Py	Car + Ser ± Chl, Py

[1)] Representative primary assemblages refer to eclogite-facies assemblages of early-Alpine age in the Sesia rocks (metapelite, orthogneiss and metabasite) and to magmatic assemblages in the andesite *s.l.* volcanics, respectively.
[2)] Minerals are listed in order of approximate decreasing abundance; abbreviations as in table 1.

brunsvigite) grow in the centre of the vein and carbonate at the rim. In the very centre, some open vugs are covered with finer-grained idiomorphic crystals of quartz.

Ore minerals are arranged as mm to cm thick irregular lenses elongated parallel to the vein direction. Pyrite forms idiomorphic fractured crystals cemented by chalcopyrite, galena, tetrahedrite and Bi-sulphosalts. On the base of semi-quantitative EDS analysis, Bi-sulphosalts show variable Bi/Pb ratio and silver enrichments. Locally, chalcopyrite and Bi-sulphosalts develop graphic-like structures, or Bi-sulphosalts occur as small veins crosscutting pyrite-chalcopyrite lenses. Hessyte (Ag_2Te), tetradymite (Bi_2Te_2S), arsenopyrite and iron-poor sphalerite ($Zn_{0.98}Fe_{0.02}S$) also rarely occur. Whilst pyrite, chalcopyrite, scheelite, tetrahedrite and rare arsenopyrite are ubiquitous, galena, Bi-sulphosalts and hessite only occur within the Passobreve area, both in the Sesia rocks and volcanics.

3.3. TYPE III VEIN SYSTEM

This vein system consists of subvertical, fine-grained carbonate, quartz ± chlorite veins striking N170–200°. Both in the Sesia Zone and volcanic rocks, they occur as up to 1 cm thick and 5 m long veins always crosscutting Type I and Type II veins (Fig. 2). They are reddish in colour and consist of carbonate (80%, ankerite: $Ca_{1.2}Mg_{0.4}Fe_{0.4}[CO_3]_2$), with minor quartz and small sulfide pods. In some places, veins become darker in colour, due to very fine-grained green chlorite (ripidolite). Within the sulfide pods, pyrite occurs as idiomorphic fractured crystals cemented by chalcopyrite and tetrahedrite with graphic-like fabric. Outside sulfide pods, chalcopyrite and tetrahedrite may also occur interstitially to carbonate and quartz.

3.4. BRECCIA PIPES

Apart from Type I to III vein systems, the hydrothermal system also comprises tourmaline-rich breccia pipes, which occur in the Scaluggia area (Fig. 2A). Three breccia pipes have been recognized in the field as elongated, lens-shaped to irregular bodies, up to two metres thick and ten metres long. While the pipe closer to the intrusion shows a broadly elliptical shape, the other two anasthomose laterally to brecciated veins that narrow laterally. At the contact with the breccia pipes, the wallrock is strongly brecciated, with abundant veinlets propagating from the pipe body. Their fabric and mineral assemblages point to a multistage evolution similar to that described in Type II vein system.

The two pipes closer to the pluton are black in colour and are characterized by rounded clasts of hydrothermal quartz (up to few millimetres in size) embedded in a fine grained tourmaline matrix. Within the clasts, quartz is strongly deformed. The matrix is composed of fine grained tourmaline alone, or in association with quartz and sulfides (pyrite, chalcopyrite and arsenopyrite). A wide range of matrix/clasts ratios, from matrix-supported to clast-supported breccias, is observed.

By contrast, the pipe further away from the pluton is reddish and is composed of irregularly

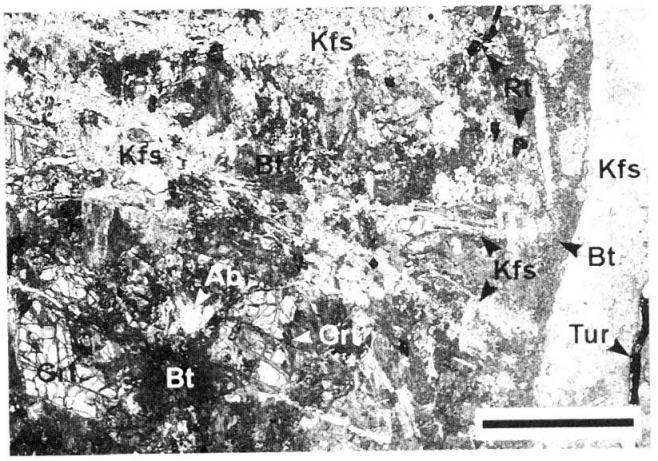

Fig. 5 Alteration assemblage associated with K-feldspar ± tourmaline Type I vein crosscutting Sesia metabasite. Part of a symmetrically zoned vein, consisting of fine-grained tourmaline and K-feldspar (in the inner and outer portions respectively) is shown on the right. Alteration assemblage consists of green biotite, K-feldspar and minor albite. Strongly fractured garnet and small crystals of rutile are the only relics of the early-alpine eclogite-facies assemblage. Sample TV293, Passobreve area, plane polarized light. Mineral abbreviations as in table 1. Scale bar is 1 mm.

shaped tourmaline ± quartz clasts (from a few millimetres to about ten centimetres in size) set in an abundant matrix of carbonate, quartz and minor pyrite, chalcopyrite and arsenopyrite (matrix-supported breccia). This matrix corresponds to the mineral assemblage occurring in Type IIc domains described above. In turn, a pre-existing brecciated fabric is preserved within the clasts and consists of brecciated tourmaline aggregates, cemented by a finer grained tourmaline + quartz matrix (Fig. 4D). Such a composite fabric closely matches the relationships between Type IIa and Type IIb domains.

In summary, based on the overall shape and composition of the clasts within pipes and brecciated veins, two types of breccias are distinguished: (i) breccias containing rounded clasts of quartz in all types of Type II domains; (ii) breccias with angular clasts composed of tourmaline in a tourmaline matrix (Type IIa), tourmaline clasts (Type IIa domains) in a tourmaline + quartz matrix (Type IIb domains), or tourmaline + quartz clasts (Type IIb domains) in a carbonate + quartz matrix (Type IIc domains).

3.5. WALLROCK ALTERATION

Hydrothermal wallrock alteration is commonly associated with all three types of vein systems. Alteration differs in both intensity and mineral assemblages according to vein types and host rock (Tab. 2).

Alteration of Type I veins develops centimetre thick pale reddish to greenish haloes. In Sesia orthogneiss and metapelite, wallrock alteration minerals consist of fine-grained Ba-rich K-feldspar ($Or_{91-93}Ab_{5-7}Cs_{1-4}$), chlorite, carbonate and minor biotite, titanite, ilmenite and pyrite. Titanite or ilmenite, the former being typical of carbonate-rich alteration domains, rim rutile. Conversely, green biotite, chlorite, green Ca-amphibole, epidote, minor K-feldspar, albite and carbonate develop in metabasite boudins (Fig. 5). Ore minerals are pyrite, magnetite and ilmenite.

Alteration of Type II vein system across Sesia metapelite and orthogneiss typically consists of centimetre thick (up to 20 cm) whitish haloes that continuously rim the vein walls. Most metamorphic minerals are completely replaced by fine-grained quartz, sericite, carbonate (ankerite: $CaMg_{0.5}Fe_{0.4}Mn_{0.1}[CO_3]_2$), with minor K-feldspar, albite, tourmaline, pyrite and rare graphite. In the inner portions of the alteration haloes, quartz is very abundant and completely overgrows the metamorphic foliation. Farther from the veins, irregular aggregates of sericite + carbonate ± K-feldspar ± albite pseudomorphically replace large flakes of metamorphic phengite. Wallrock alteration in the Sesia eclogite is given by centimetre thick whitish haloes, mainly consisting of chlorite and fine grained calcite. Chlorite aggregates occur as pseudomorphs after metamorphic garnet. Minor barium-enriched K-feldspar ($Or_{90-98}Ab_{1-9}Cs_1$), albite ($Or_{0-2}Ab_{96-99}An_{0-2}$), quartz, tourmaline, ilmenite, titanite and pyrite also occur. Alteration of Type II vein system in the andesite *s.l.* volcanics consists of carbonate, quartz, chlorite and very minor pyrite.

The hydrothermal alteration of Type III veins is very minor and only mm thick. Alteration minerals include carbonate and sericite, with minor chlorite and pyrite. Titanite also occurs in the Sesia metapelite and orthogneiss.

4. Composition of tourmaline, chlorite and arsenopyrite

Chemical analyses of minerals were performed using a Cambridge S360 electron microscope connected to a Link QX2000 energy dispersive system. Operating conditions were 15 kV acceleration voltage, beam current 50 nA and 50 s counting time. Natural and synthetic minerals were used as standards. A ZAF-4 correction procedure was performed on-line, and cation distribution in most minerals was calculated off-line using the

Tab. 3 Representative chemical compositions of tourmaline from different vein systems.

	Type I vein system		**Type II vein system**							
			coarse-grained Tur in IIa domains		fine-grained Tur in IIa domains			IIb domains		
	core	rim	core	rim	core	intermediate	rim	core	int	rim
Sample	*d12-4-tr1core*	*d12-4-tr1rim*	*289-1/torm*	*289-1torm3*	*241-5-tr8a*	*241-5-tr8b*	*241-5-tr8c*	*289-1 tr4a*	*289-1tr4b*	*289-1-tr4c*
SiO_2	33.77	35.03	35.85	35.99	35.91	34.99	35.97	36.58	36.59	35.64
Al_2O_3	23.63	26.60	28.59	26.78	28.47	24.54	27.97	30.23	27.31	24.12
TiO_2	0.00	0.69	1.92	1.11	0.11	0.19	0.50	0.20	1.01	0.87
FeO_{tot}	17.87	12.68	5.86	8.86	12.75	16.36	12.75	6.86	8.86	14.82
MnO	0.11	0.00	0.00	0.00	0.00	0.00	0.00	0.00	0.07	0.00
MgO	3.89	5.05	7.82	7.04	5.38	4.94	5.65	7.55	7.21	6.08
CaO	0.32	0.68	1.40	1.34	0.40	0.49	0.75	0.26	1.27	1.39
Na_2O	2.43	2.42	1.87	2.07	2.92	2.64	2.51	2.64	2.26	2.16
K_2O	0.01	0.17	0.01	0.01	0.02	0.04	0.00	0.00	0.00	0.00
Total	82.36	83.32	83.50	83.05	86.06	84.20	86.09	84.33	84.69	85.07
Si	6.22	6.15	6.05	6.20	6.10	6.22	6.10	6.11	6.19	6.23
Al^{IV}	0.00	0.00	0.00	0.00	0.00	0.00	0.00	0.00	0.00	0.00
Al^{VI}	5.13	5.51	5.69	5.44	5.70	5.14	5.59	5.95	5.45	4.97
Ti	0.00	0.09	0.24	0.14	0.01	0.03	0.06	0.02	0.13	0.11
Fe^{2+}	2.76	1.87	0.83	1.25	1.71	1.78	1.71	0.96	1.25	1.68
Fe^{3+}	–	–	–	–	0.10	0.65	0.10	0.00	0.00	0.49
Mn	0.02	0.00	0.00	0.00	0.00	0.00	0.00	0.00	0.01	0.00
Mg	1.07	1.32	1.97	1.81	1.36	1.31	1.43	1.88	1.82	1.58
Total *R*2	3.84	3.27	3.03	3.20	3.18	3.77	3.30	2.86	3.21	3.86
Ca	0.06	0.13	0.25	0.25	0.07	0.09	0.14	0.05	0.23	0.26
Na	0.87	0.82	0.61	0.69	0.96	0.91	0.82	0.86	0.74	0.73
K	0.00	0.04	0.00	0.00	0.00	0.01	0.00	0.00	0.00	0.00
Total *R*1	0.93	0.96	0.87	0.94	1.04	1.01	0.96	0.90	0.97	0.99
Fe/(Fe+Mg)	0.72	0.59	0.30	0.41	0.57	0.65	0.56	0.34	0.41	0.58
Fe^{2+}/Fe_{tot}	–	–	–	–	0.95	0.73	0.94	1.00	1.00	0.77

Fe^{3+} contents in both fine-grained tourmaline from Type IIa domains and tourmaline from Type IIb domains calculated according to LYNCH and ORTEGA (1997), see text for discussion.

approaches of AFIFI and ESSENE (1988) and ULMER (1993).

Only analytical data on tourmaline, chlorite and arsenopyrite are reported here, as the compositional range of the other analyzed phases has been reported in the previous section. Particularly, the mineral chemistry of tourmaline is discussed in detail, because tourmaline abundance is one of the peculiar features of this hydrothermal system. Moreover, the extreme compositional range possible makes tourmaline a useful petrogenetic indicator (HENRY and GUIDOTTI, 1985). Mineral chemical data of chlorite and arsenopyrite are also reported, and their composition is then used in geothermometric estimates.

4.1. TOURMALINE

According to LONDON and MANNING (1995) and LYNCH and ORTEGA (1997), a site-reference scheme of tourmaline may be represented by $(R1)(R2)_3(R3)_6(BO_3)_3Si_6O_{18}(OH,F,O)_4$, where $R1$ = Na, Ca, K, or vacant; $R2$ = Fe^{2+}, Mg, Mn^{2+}, and Fe^{3+}, Cr^{3+}, V^{3+}, Ti^{4+}, or Al (when $R1$ is vacant), or Li (when coupled with Al); and $R3$ = Al, Fe^{3+}, Cr^{3+}, V^{3+}, and Fe^{2+} or Mg (when coupled with Ca substitution in $R1$), or $1.33Ti^{4+}$. Exchange vectors of tourmaline have been discussed by BURT (1989), HAWTHORNE (1996) and HENRY and DUTROW (1996). In the absence of direct analysis of B, O, H and F, the ZAF-corrected microprobe analyses of tourmaline were treated following the method described by HENRY and DUTROW (1996). Assuming both boron and OH as stoichiometric (B = 3 and OH = 4 atoms p.f.u., respectively), analyses have been normalized to 24.5 oxygens. Representative analyses of tourmalines from Types I, IIa and IIb veins are given in table 3, and all analyses are plotted in figures 6 and 7.

Tourmalines from all vein types are dravite–schorl–povondraite–uvite solid solutions according to HENRY and DUTROW (1996), characterized by high silicon contents ($6.05 < Si < 6.37$ atoms

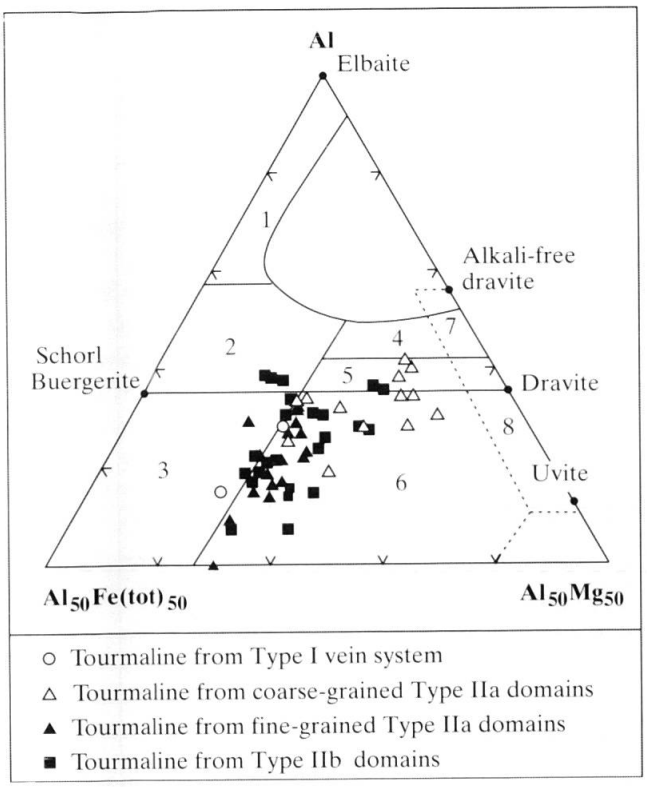

Fig. 6 Al–Fe_{tot}–Mg ternary diagram for tourmalines from Type I and Type II vein systems. Compositional range of tourmaline from different rock types (HENRY and GUIDOTTI, 1985) are: (1) Li-rich granitoids, pegmatites and aplites; (2) Li-poor granitoids, pegmatites and aplites; (3) hydrothermally altered granitic rocks; (4) metapelites and metapsammites coexisting with an Al-saturating phase; (5) metapelites and metapsammites not coexisting with an Al-saturating phase; (6) Fe^{3+}-rich quartz-tourmaline rocks, calc-silicates and metapelites; (7) low-Ca ultramafics and Cr, V-rich metasediments; (8) metacarbonates and metapyroxenites.

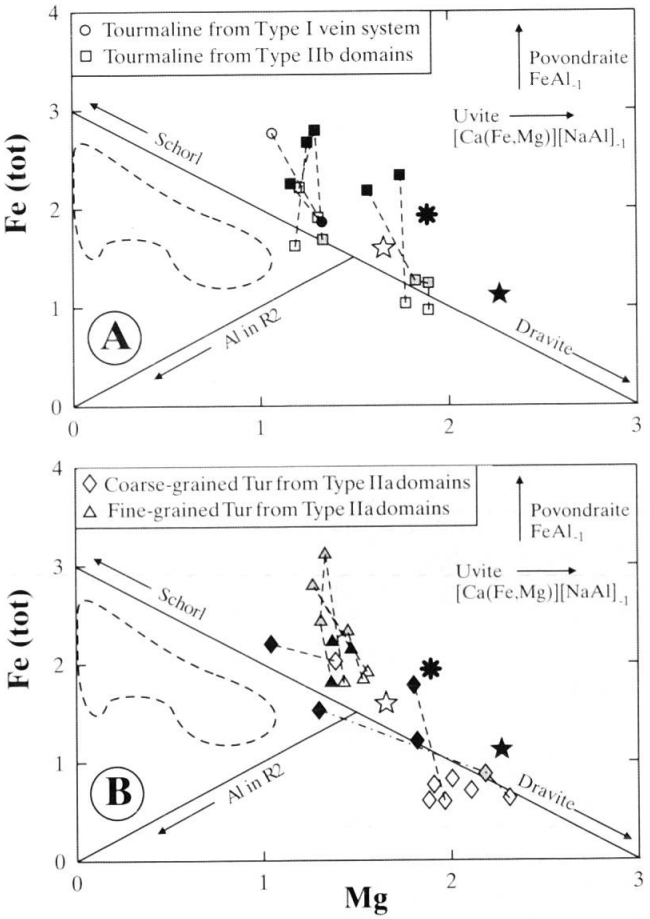

Fig. 7 Fe–Mg diagrams for tourmaline from Type I and Type II vein systems. Open and full symbols refer to core and rim compositions, respectively. Some intermediate compositions between core and rim are given by symbols with grey filling. Arrows emphasize trends toward end-member compositions as well as the occurrence of Al in *R*2 site. Average compositions of tourmalines from Los Bronces (open star), El Teniente (full star), and Coxhealth deposits (asterisk) are shown as reference (LYNCH and ORTEGA, 1997). The dashed line encloses the compositional field of tourmaline from Cornwall S-type granites and associated hydrothermal rocks (LONDON and MANNING, 1995).

p.f.u., av. = 6.16), with Si contents being higher than the theoretical site occupancy. It is worth noting that tourmaline analyses with silicon in excess of 6.0 atoms p.f.u. have been reported (DEER et al., 1986; JIANG et al., 1995). By contrast, aluminum contents are often lower than *R3*-site theoretical occupancy ($4.42 < Al < 6.01$ atoms p.f.u., av. = 5.38), and wide ranges in Fe, Mg, and Na content have been observed ($0.63 < Fe_{tot} < 3.12$ atoms p.f.u., av. = 1.89; $1.01 < Mg < 2.27$, av. = 1.46; $0.57 < Na < 0.96$, av. = 0.78). Calcium is relatively low ($0.02 < Ca < 0.38$, av. = 0.16), and potassium content is almost negligible (≤ 0.11 atoms p.f.u.). These variations in chemical composition (particularly of Al, Fe and Mg) reflect both different occurrence and crystal zoning (Figs 6 and 7). On the contrary, Ca and Na cannot be related to different vein systems or zoning patterns. In the Al–Fe_{tot}–Mg ternary diagram of figure 6 (HENRY and GUIDOTTI, 1985), tourmalines fall in rock type fields which are compatible with the host rocks occurring at Passobreve and Scaluggia. Notably, most core compositions fall within the fields of metapelites and metapsammites, whilst rim compositions trend towards iron-richer compositions (Fig. 7).

Tourmaline from Kfs ± Tur Type I veins is a dravite–schorl–povondraite solid solution. On average this tourmaline is the Fe-richest ($1.86 < Fe < 2.75$; av. = 2.30), with low Al and Mg contents ($5.13 < Al < 5.51$, av. = 5.29; $1.07 < Mg < 1.32$, av. = 1.21) and very low Ca content ($0.06 < Ca < 0.13$; av. = 0.10). It is patchily zoned, with irregular Fe-richer cores mantled by thin Al- and Mg-richer rims.

Coarse grained tourmaline in Tur ± Qtz Type IIa domains is a dravite–schorl–uvite solid solu-

Tab. 4 Representative chemical compositions of chlorite from different vein systems.

	Type I		Type IIb		Type IIc		Type III
Sample	*299-4-4*	*299-3-4*	*292-2-3*	*292-2-4*	*344-2-3*	*344-5-3*	*D16-3/1*
SiO_2	28.28	26.04	27.16	25.83	25.21	24.94	26.43
TiO_2	0.05	0.18	0.00	0.19	0.06	0.00	0.33
Al_2O_3	17.17	18.15	18.60	19.12	18.12	20.28	17.76
Fe_2O_3	0.67	2.59	1.33	2.71	1.21	1.94	1.28
FeO	29.32	29.61	25.22	25.60	37.03	29.76	31.50
MnO	0.24	0.39	0.00	0.14	0.16	0.46	0.59
MgO	11.16	11.37	14.80	13.68	6.36	10.60	10.85
CaO	0.17	0.02	0.00	0.06	0.11	0.01	0.08
Na_2O	0.66	0.59	0.76	0.67	0.63	0.61	0.45
K_2O	1.13	0.16	0.00	0.07	0.00	0.00	0.14
H_2O	11.19	11.14	11.36	11.26	10.73	11.10	10.64
Total	100.04	100.24	99.23	99.34	99.62	99.71	100.05
Si	6.06	5.60	5.74	5.50	5.64	5.39	5.70
Ti	0.01	0.03	0.00	0.03	0.01	0.00	0.05
Al^{IV}	1.94	2.40	2.26	2.50	2.36	2.61	2.30
Al^{VI}	2.40	2.02	2.36	2.30	2.42	2.55	2.21
Fe^{3+}	0.11	0.64	0.21	0.44	0.20	0.32	0.21
Fe^{2+}	5.26	5.25	4.45	4.56	6.92	5.38	5.68
Mn	0.04	0.15	0.00	0.03	0.03	0.08	0.11
Mg	3.57	3.68	4.65	4.34	2.12	3.41	3.49
Ca	0.04	0.01	0.00	0.01	0.03	0.00	0.02
Na	0.27	0.25	0.31	0.28	0.27	0.26	0.19
K	0.31	0.04	0.00	0.02	0.00	0.00	0.04
OH	16.00	16.00	16.00	16.00	16.00	16.00	16.00
X_{Mg}	0.40	0.39	0.50	0.46	0.24	0.38	0.37

Cations are calculated on the basis of 20 cations and 36 oxygens assuming stoichiometry and charge balance (ULMER, 1993). $X_{Mg} = Mg/(Mg + Fe_{tot})$.

tion. On average, it is enriched in Al ($5.18 < Al < 6.01$, av. = 5.59), Mg ($1.01 < Mg < 2.27$, av. = 1.77) and Ca ($0.07 < Ca < 0.38$; av. = 0.23) with respect to all the other tourmalines from VDC. The wide variation in Mg is inversely related to the Fe contents ($0.63 < Fe < 2.19$, av. = 1.19). Cores are richer in Mg and Al than rims.

Fine-grained tourmaline in Tur ± Qtz Type IIa domains is a dravite–schorl–povondraite solid solution. On average, it is Fe-richer ($1.71 < Fe < 3.12$, av = 2.16), and Mg- and Al-poorer than coarse grained tourmaline. Compositional ranges of both Fe and Al ($4.42 < Al < 5.82$, av. = 5.25) are rather wide, whilst Mg content is relatively constant ($1.27 < Mg < 1.56$, av. = 1.38). Crystals show a discontinuous oscillatory zoning, with subhedral cores and thin outer rims enriched in Al, and Fe-rich inner rims. The Ca content is low ($0.07 < Ca < 0.20$; av. = 0.14). Tourmaline from Tur + Qtz Type IIb domains shows the most extensive range in dravite–schorl–povondraite-uvite solid solution ($4.68 < Al < 5.96$, av. = 5.40; $0.96 < Fe < 2.78$, av. = 1.88; $1.17 < Mg < 1.91$, av. = 1.45). Moreover, although calcium is low on average ($0.02 < Ca < 0.35$; av. = 0.15), some spot analyses show Ca contents as high as those of coarse-grained Type IIa tourmaline. Crystals are zoned, with Al-rich cores and Fe-rich rims, whilst Mg contents are rather constant within single grains.

Compositions of tourmalines from selected porphyry Cu ± Mo ± Au deposits and Cornwall S-type granites (LONDON and MANNING, 1995; LYNCH and ORTEGA, 1997) are also shown in figure 7. Compared with tourmaline from the porphyry deposits, average compositions of tourmaline from VDC hydrothermal system are similar to those from Los Bronces (and partly to those from Coxhealt). Tourmaline from El Teniente is dravite-richer and can be only compared to core compositions of coarse-grained tourmaline from Type IIa domains. Conversely, tourmaline from Cornwall S-type granites and associated hydrothermal rocks is Mg-poorer (and Al-enriched), tending more towards the schorl end-member.

Crystal-chemical features of tourmaline can be hardly modelled on the base of the above analyses (for a discussion, see: HAWTHORNE, 1996; HENRY and DUTROW, 1996; HAWTHORNE and

HENRY, 1999). However, textures and zoning patterns discussed above discouraged X-ray investigations on single tourmaline grains. The lack of data on H, Li, B and Fe^{3+} contents in tourmaline limits the use of the classification scheme recently proposed by HAWTHORNE and HENRY (1999), but some further points deserve a short discussion.

Total occupancy of *R*1, *R*2, *R*3 sites plus tetrahedral site of VDC tourmaline ranges between 15.65 and 16.26 (av. = 15.95). The *R*1 site is occupied by Na and minor Ca ($0.72 < R1 < 1.09$, av. = 0.95), showing the occurrence of some vacancy as extensively reported for tourmaline elsewhere (DEER et al., 1986; HENRY and DUTROW, 1996). About *R*2 and *R*3 sites, different models have been proposed for the distribution of divalent and trivalent cations (LONDON and MANNING, 1995; HENRY and DUTROW, 1996; LYNCH and ORTEGA, 1997). According to HENRY and DUTROW (1996) and LYNCH and ORTEGA (1997), the total occupancy of the *R*2 site (*R*2 = Mg + Mn + Fe + Ti) is commonly higher than 3 atoms p.f.u. The average *R*2 contents of tourmaline from all vein systems ($2.60 < R2 < 4.61$, av. = 3.40) are in agreement with those shown by Al-poor tourmalines (HENRY and DUTROW, 1996) (Figs 6 and 7). Only some core compositions from Type IIa (4 spot analyses) and Type IIb (3 spot analyses) tourmalines suggest some deficiency in the *R*2 site, which may be filled by Li. However, Al-poor compositions are not compatible with significant amount of lithium in the *R*2 site (HENRY and DUTROW, 1996).

All normalization procedures allocate Al in the tetrahedral site (if some Si deficiency occurs) and then in the *R*3 site. In the Al-poor VDC tourmalines, the *R*3 site cannot be filled by aluminum alone, hence other trivalent cations (and possibly Mg) occur in *R*3 (HENRY and DUTROW, 1996). On the basis of negative correlation between Fe and Al, LYNCH and ORTEGA (1997) suggest that both Fe^{2+} and Fe^{3+} fill the *R*3 deficiency. They suggest that the amount of Fe^{3+} in *R*3 is controlled by the coupled substitution of Ca in *R*1, according to the relation:

$$Fe^{3+}\ (R3) = Fe–(3–Mg)–Ca \qquad (1)$$

Such a negative correlation between iron and aluminum only occurs in Type IIb and fine-grained Type IIa tourmalines. Using relation (1), the $Fe^{3+}/(Fe^{2+} + Fe^{3+})$ value in fine-grained Type IIa tourmaline ranges from 0.00 to 0.40 (av. = 0.17), whilst in Type IIb tourmaline it ranges from 0.00 to 0.31 (av. = 0.10). Following the above reasoning, relation (1) should not be used for Type I and coarse-grained Type IIa tourmalines. However, a low Fe^{3+} value is assumed, as they show the highest occupancies of Al in the *R*3 site.

4.2. CHLORITE

Analyses were performed on chlorite from different vein types, and selected compositions are given in table 4.

Minor chlorite occurring near vein walls in K-feldspar ± tourmaline Type I vein system is a brunsvigite-ripidolite (HEY, 1954), and is characterized by a wide range in silicon contents ($5.52 < Si < 6.06$ atoms p.f.u., av. = 5.75). Conversely, it shows a narrow range of $Mg/(Mg + Fe_{tot})$ ratio (0.37–0.40, av. = 0.39). Al contents range between 4.25 and 4.75 atoms p.f.u. (av. = 4.45).

Chlorite from Type IIb domains is a ripidolite-pycnochlorite. The silicon contents range between 5.50 and 5.74 atoms p.f.u. (av. = 5.62), Al between 4.62 and 4.80 atoms p.f.u. (av. = 4.71). The $Mg/(Mg + Fe_{tot})$ ratio ranges between 0.39 and 0.51 (av. = 0.48).

Chlorite from Type IIc domains is a ripidolite–brunsvigite. The silicon contents range between 5.39 and 5.64 atoms p.f.u. (av. = 5.52), and Al between 4.78 and 5.28 (av. = 4.98). Type IIc chlorite is Fe-richer than those occurring in Type IIb assemblage, and its $Mg/(Mg + Fe_{tot})$ ratio ranges between 0.23 and 0.48 (av. = 0.36).

The fine-grained chlorite from tourmaline-free Type III vein system (one spot analysis) is a brunsvigite, and shows Si and Al contents of 5.70 and 4.51, respectively. The $Mg/(Mg + Fe_{tot})$ ratio is 0.37.

4.3. ARSENOPYRITE

Compositions of arsenopyrite have been determined, as they may provide useful information on sulfur fugacity and possibly temperature (KRETSCHMAR and SCOTT, 1976; SHARP et al., 1985). Spot analyses have been performed on both disseminated idiomorphic grains and anhedral inclusions in pyrite. Composition of each crystal has been averaged from spot analyses, in order to minimize the composition-morphology dependencies discussed by KERESTEDJIAN (1997).

Arsenopyrites from Type IIb domains in breccia pipe at Scaluggia fall into two different compositional groups. Disseminated subhedral arsenopyrite in equilibrium with pyrite shows the highest As content (31.81–32.50 at%, av. = 32.12). Conversely, the As content of anhedral arsenopyrite included in pyrite is much lower (30.29–31.24 at%, av. = 30.67). The As content of arsenopyrite from Type IIc domains within a breccia pipe at Scaluggia has a narrow compositional range, between 31.78 and 32.07 at% (av. = 31.90), which is similar to that of lower-As Type IIb disseminated arsenopyrite. In Type IIc vein domains at Passo-

breve, the As contents of arsenopyrite range from 31.34 to 31.68 at% (av. = 31.49).

5. Discussion

5.1. RELATIONSHIPS WITH THE VALLE DEL CERVO INTRUSION

Field relationships and petrography of the tourmaline-rich ore-bearing rocks from the lower VDC show that they are part of a complex hydrothermal system cropping out within the Sesia Zone and its volcano-sedimentary cover. Many lines of evidence suggest a close relationship between the hydrothermal activity and the VDC Pluton. They include:

(1) Their spatial proximity. The same relationship between plutonic activity and tourmaline-rich hydrothermal rocks is also observed in other portions of the Sesia Zone south to east of the plutonic body including the Sessera valley, Cima Cucco and Pian del Lotto (AQUATER, 1994). As discussed above, the Sesia rocks between the VDC Pluton and the Insubric Line broadly represent the roof of the VDC intrusion.

(2) The abundance of tourmaline in the hydrothermal system, reflecting high boron concentrations in the fluids. Ore-bearing tourmaline-rich veins and breccia pipes associated with plutonic activity have been reported from different localities, including the Andean Cordillera (SILLITOE and SAWKINS, 1971; SHELNUTT and NOBLE, 1985; WARNAARS et al., 1985), Cornwall (CHAROY, 1982; LONDON and MANNING, 1995) and Queensland (BAKER and ANDREWS, 1991). The development of tourmaline (and possibly dumortierite) is generally considered to reflect the availability of magmatic and magmatic-derived boron during the crystallization of related granitoids (SLACK, 1996). In fact, in magmatic systems boron behaves as an incompatible element and is therefore progressively concentrated in residual melts, until a buffering crystal-melt equilibrium is established, or an aqueous phase is exsolved from the melt (LONDON et al., 1996). According to the available experimental data, in presence of a vapor phase boron slightly partitions in favor of the vapor (PICHAVANT, 1981; LONDON et al., 1988). A much stronger partitioning is expected, however, at very high water/melt mass ratios, corresponding to the very late stages of crystallization (LONDON et al., 1996).

In the VDC and surrounding areas, boron is heterogeneously distributed (RIMIN, 1989; AQUATER, 1994). In the VDC intrusion, the monzonitic and syenitic rocks show "typical" boron contents (mostly in the range 20–60 ppm, with maxima around 180 ppm), whilst the granodioritic core is boron-depleted, with values mostly below 20 ppm. On the contrary, RIMIN (1989) reported the occurrence of a strong positive boron anomaly (up to tens of thousands ppm), broadly striking NE–SW in the Sesia rocks southeast (i.e. in the roof) of the VDC intrusion. Maxima are centered in areas characterized by hydrothermal evidences (Passobree and Scaluggia along the Cervo river; Pian del Lotto in the Oropa valley; Orio del Mosso, north of Bogna; Fig. 1).

(3) The abundance of hydrothermal breccias, particularly in the area closer to the plutonic body. Breccia pipes are a typical feature of shallow level magmatic-hydrothermal systems (SILLITOE, 1985), possibly related to violent escape of overpressurized fluids exsolved during the latest stages of magmatic crystallization (BURNHAM, 1979).

(4) The typology and distribution of the hydrothermal mineralizations. In the studied system, the ore assemblages (and particularly the occurrence of thorite, scheelite, hessyte and Bi-sulphosalts) are in agreement with a connection between hydrothermal system and late-magmatic activity. Moreover, considering the VDC Pluton and host rocks, a broadly concentric zonation of the mineralizations exists, with W and especially Mo concentrated within the granodiorite core, while Cu, Pb, Zn, Ag, Au, Sb and Bi mostly occur in the outer portions of the body and in the host rocks (Fig. 1; AQUATER, 1994). This type of zonal arrangement is typically found in hydrothermal systems genetically and spatially related to plutonic activity (e.g., STONE and EXLEY, 1986).

Even so, a connection between hydrothermal activity and brittle deformation cannot be ruled out in the lower VDC. The andesite volcanics and volcanoclastics are extensively tectonized, and movements along the Insubric line are possibly responsible for (re-)mobilization of vein material at least in the upper, tourmaline-poor part of the hydrothermal system.

5.2. P-T-X_{FLUID} CONSTRAINTS OF THE HYDROTHERMAL SYSTEM

The tourmaline-rich ore-bearing veins and breccia pipes of the lower VDC consist of multistage hydrothermal assemblages. Lithostatic pressure and temperature have certainly controlled their precipitation, but chemical composition and physical properties of the coexisting hydrothermal fluid (possibly changing with time and space) were also important constraints.

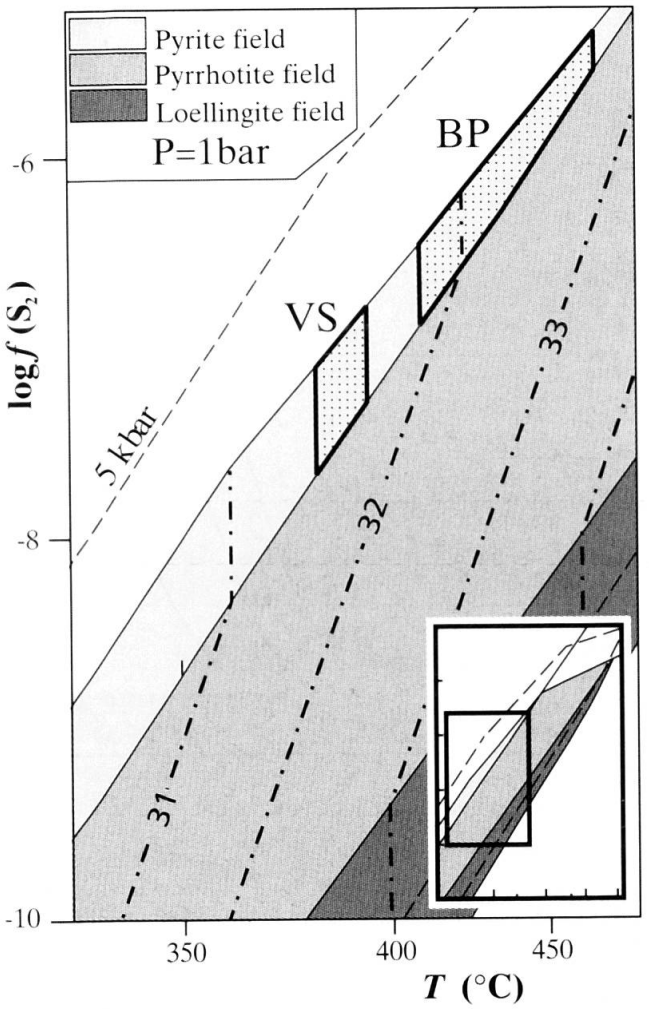

Fig. 8 Detail of T versus logfs_2 diagram of the Fe–As–S system, showing the stability field of arsenopyrite in equilibrium with pyrite, pyrrhotite and loellingite, respectively (SHARP et al., 1985). The inset shows the complete phase diagram. Isopleths (dashed-dotted lines) are labelled according to As content (at%) in arsenopyrite. Dashed lines depict shift of arsenopyrite stability field at 5 kbar. The BP and VS dotted fields refer to Type IIb plus Type IIc domains in breccia pipes from Scaluggia area, and Type IIb vein domains from Passobreve area, respectively.

Precise P-T modeling of fluid-mineral equilibria would require that either composition(s) of hydrothermal fluid(s) be independently known, or that low-variance mineral assemblages occur. For example, GAROFALO et al. (2000) recently derived and tested thermodynamic properties of tourmaline end-members with data of well-constrained samples from the Mole Granite (Australia) magmatic-hydrothermal system. These data included independently estimated temperature and composition (by way of quantitative LA-ICP-MS analyses and microthermometry of fluid inclusions) of boron-rich hydrothermal fluid in equilibrium with low-variance Kfs–Ab–Ms–Qtz–Tur assemblage.

At present, chemical and physical properties of hydrothermal fluid(s) in the lower VDC are poorly known (see below), and most of the hydrothermal mineral assemblages are high-variance assemblages. However, some preliminary P-T-X_{fluid} estimates that broadly constrain the hydrothermal system are given below on the base of arsenopyrite and chlorite geothermometry, petrologic analysis of mineral assemblages in the thermal aureole of the VDC Pluton, available geologic data and fluid inclusion petrography.

Arsenopyrite geothermometry

Arsenopyrite geothermometer, based on the relationship between As contents of arsenopyrite, fs_2 and temperature, was calibrated experimentally by KRETSCHMAR and SCOTT (1976) and modified by SHARP et al. (1985). The reliability of the arsenopyrite geothermometer is a matter of debate, as its applications have often given conflicting results, probably due to disequilibrium phenomena (SHARP et al., 1985). In particular, KERESTEDJIAN (1997) pointed out a dependence of the composition on morphology within single arsenopyrite crystals. In order to minimize these compositional heterogeneities, we averaged different spot analyses within single crystals for the application of the geothermometer.

Arsenopyrite from different domains in Type II vein system and breccia pipes is always associated with pyrite. This constrains temperature and sulphur fugacity to the narrow stability field of arsenopyrite + pyrite (Fig. 8). On the basis of the As contents, different T–fs_2 ranges are obtained. A first range ($415 < T < 465$ °C, $-6.8 < \log fs_2 < -5.3$) is given by disseminated subhedral arsenopyrite in both Type IIb and IIc domains from breccia pipes at Scaluggia (BP field in figure 8). A second range ($380 < T < 395$ °C, $-7.7 < \log fs_2 < -6.7$) is given by disseminated subhedral arsenopyrite in Type IIc vein domains at Passobreve (VS field in figure 8). It is worth noting that higher temperatures are obtained for breccia pipes from the Scaluggia area (i.e., closer to the intrusive contact), whilst lower temperature estimates correspond to vein system occurring farther from the intrusive contact in the Passobreve area. Temperatures would be slightly higher when taking into account the effect of total pressure on the geothermometer (Fig. 8 and SHARP et al., 1985).

The geothermometer has also been applied to anhedral arsenopyrite included in pyrite within Type IIb domains in breccia pipe at Scaluggia, though microstructural relationships suggest that arsenopyrite formed earlier than pyrite. The calculated range ($325 < T < 370$ °C, $-9.5 < \log fs_2 < -7.5$, not shown in figure 8) is significantly different

from that obtained in the same breccia pipe for subhedral arsenopyrite in equilibrium with pyrite.

Chlorite geothermometry

Empirical chlorite geothermometers are mainly based on the correlation between Al^{IV} and temperature (CHATELINEAU and NIEVA, 1985; CHATELINEAU, 1988; JOWETT, 1991), whilst a six-component solid solution model has been proposed by WALSHE (1986; see also DE CARITAT et al., 1993, for a discussion).

The calibrations of CHATELINEAU and NIEVA (1985), WALSHE (1986), CHATELINEAU (1988) and JOWETT (1991) have been applied to chlorites from different Type II and Type III veins at Passobreve. However, the calibration of WALSHE (1986) gives a wide and unrealistic range of low temperatures (≤ 230 °C, when applied to chlorite from any vein type) and will not be further considered. Chlorite from Type I veins has not been considered, as it occurs at vein walls and possibly belongs to alteration assemblages.

Average temperatures from chlorite in Type IIb veins are: 275 °C (CHATELINEAU and NIEVA, 1985), 330 °C (CHATELINEAU, 1988) and 410 °C (JOWETT, 1991). Average temperatures from chlorite in Type IIc veins are: 280 °C (CHATELINEAU and NIEVA, 1985), 340 °C (CHATELINEAU, 1988) and 420 °C (JOWETT, 1991). Temperatures from chlorite in Type III veins are: 250 °C (CHATELINEAU and NIEVA, 1985), 310 °C (CHATELINEAU, 1988) and 390 °C (JOWETT, 1991).

These values must be considered with caution, because none of the above calibrations is experimental and "no single chlorite geothermometer performs satisfactorily over the whole range of natural conditions" (DE CARITAT et al., 1993; WALSHE, 1998, pers. com). Nevertheless, each single geothermometer gives very similar temperatures for Type IIb and IIc chlorites, and slightly lower temperatures (of about 20–30 °C) for Type III chlorite.

A comparison of temperature estimates obtained from the arsenopyrite and the chlorite geothermometers is only possible in Type IIc veins from Passobreve. For these veins, arsenopyrite geothermometry gives T = 380–395 °C, whilst chlorite geothermometry yields a wider range of temperatures, depending on different calibrations. Only the calibration of JOWETT (1991) gives values broadly close to the arsenopyrite T estimates. Since: (i) the arsenopyrite geothermometer is based on both experimental calibration and theoretical ground, and (ii) the composition of hydrothermal arsenopyrite is thought to be less sensitive to later re-equilibration, temperature estimates from the arsenopyrite geothermometry are likely to be closer to actual temperature of the hydrothermal system.

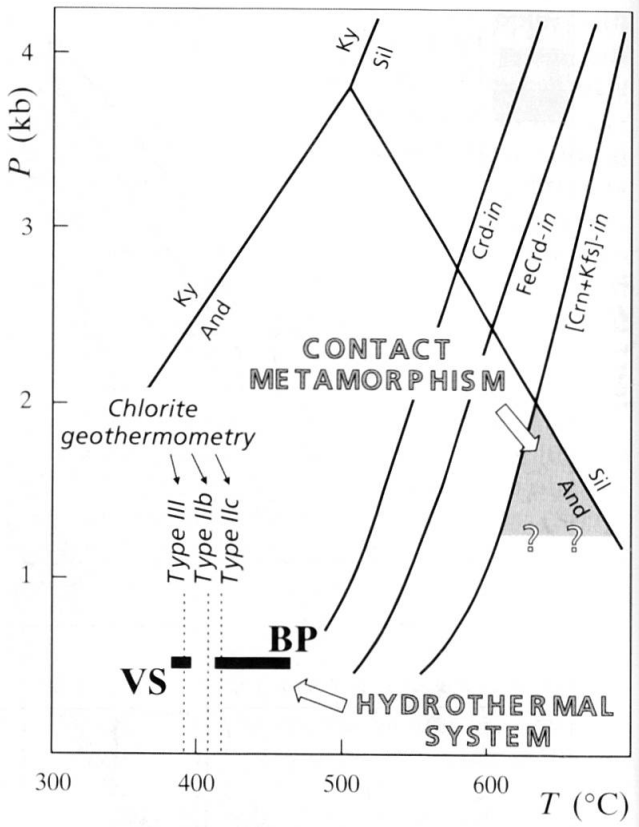

Fig. 9 Estimated *P-T* conditions of contact metamorphism due to the intrusion of VDC Pluton in the Sesia host rocks at $P_{tot} = P(H_2O)$, and summary of *P-T* constraints for the lower VDC hydrothermal system. Selected equilibria in the KNASH model system bracket (grey area) the breakdown of muscovite to corundum + K-feldspar within the stability field of both andalusite and cordierite, as described by FORNASERO (1978) in the thermal aureole. Dashed lines refer to temperature estimates of hydrothermal Type II and III vein systems based on the chlorite geothermometer of JOWETT (1991). The two bars are temperature estimates according to arsenopyrite compositions in both vein system (VS) and breccia pipe (BP) from figure 8. Bars have been approximately located at the lithostatic pressure (P = 0.5 kbar) discussed in text. Mineral abbreviations according to table 1.

Pressure estimates

Pressure estimates for the emplacement of the hydrothermal system are not constrained by any vein or breccia pipe mineral assemblage. However, some constraints on the lithostatic pressure are given by its close relationships with the VDC intrusion.

A minimum pressure value is given by the current thickness of the Sesia rocks, which were originally overlying the VDC stock. Restoring the VDC crustal section to its primary position (LANZA, 1977, 1979, 1984), a lithostatic pressure of about

250 bars is obtained for the intrusive contact at Bogna. However, the actual thickness of Sesia rocks in the roof of the pluton is not exactly known, and this pressure value could be underestimated.

Further constraints are given by FORNASERO (1978), who documented the widespread occurrence of andalusite and cordierite in the thermal aureole of the plutonic body. He also reported the occurrence of corundum + K-feldspar pseudomorphs after white mica in quartz-free domains in one sample from the aureole northwest of the pluton (Val Pragnetta). Based on phase equilibria analysis, FORNASERO (1978) suggests that the development of the Crn + Kfs assemblage in the andalusite stability field occurred at $P \leq 1.5$ kbar and $T \leq 670$ °C.

In order to revise these estimates, selected phase equilibria in the KNASH model system were calculated using the approach of CONNOLLY (1990) and CASTELLI et al. (1997), and solid solution models of CONNOLLY et al. (1994). The thermodynamic properties of solid phases (K-feldspar, albite, muscovite, paragonite, quartz, corundum, diaspore, and the three Al_2SiO_5-polymorphs) and aqueous fluid included in the model system were taken from HOLLAND and POWELL (1998). The analysis of univariant reactions: Ms = Kfs + Crn + H_2O and And = Sil shows that, with increasing temperature, the breakdown of muscovite to corundum + K-feldspar may occur in the stability field of andalusite up to $P = 2$ kbar (Fig. 9). Slightly higher pressures (up to ~2.5 kbar) are expected when considering the effect of NaK_{-1} exchange in both mica and feldspar. FORNASERO (1978) also reports the occurrence of scanty sillimanite around andalusite in the same sample from Val Pragnetta. This sillimanite may be explained by either the deeper position of Val Pragnetta rocks, or the thermal climax reached during the prograde thermal path related to the intrusion. In any case, the abundance of well preserved andalusite suggests that temperature hardly exceeded the upper thermal stability limit of andalusite, preventing its breakdown. As a consequence, the maximum depth for the Crn + Kfs assemblage in Val Pragnetta would be ~ 7.5 km at 630 °C (Fig. 9).

The topographic distance between Val Pragnetta and the southeastern margin of the pluton (Fig. 1) is around 6.5 km, which would correspond to a thickness of the plutonic body (tilted to its original position) of around 5.6 km. As a consequence, a depth broadly ranging between 7.5 km (Val Pragnetta) and 2 km (Bogna) is obtained for the VDC intrusion. Such a depth is in agreement with the tabular fabric of plagioclase in the granodiorite core, which suggests magma emplacement at relatively shallow level (CALLEGARI, 1999, pers. com.), as also indicated by BIGIOGGERO et al. (1994). Assuming lithostatic pressure, a maximum depth of about 2 km (corresponding to a pressure around 500 bars) is therefore suggested for the deepest parts of the VDC hydrothermal system close to the upper intrusive contact.

Constraints on fluid composition

A thorough characterization of fluid inclusion populations in the lower VDC hydrothermal system is difficult. Multistage brecciation and very fine grain size allowed only petrographic analysis of fluid inclusions.

The only primary fluid inclusions occur in quartz from Type IIc and Type III veins, as very small liquid-rich, aqueous two-phase (liquid + vapor, L + V) inclusions arranged along growth zones. Three-phase, salt-bearing fluid inclusions are notably absent in Type IIc and Type III veins.

Older veins are either void of fluid inclusions, or mostly contain very small liquid-rich, L + V inclusions, which are secondary, or of uncertain origin. Some three-phase inclusions (L + V + salt) however occur in quartz within both Type IIa and Type IIb veins (and in breccia pipes) and occasionally in K-feldspar in Type I veins. The latter are also characterized by the occurrence of vapor-rich (vapor + liquid and vapor-only) inclusions. Finally, all vein systems retain abundant L + V inclusions of clear secondary origin.

These data suggest that a fluid evolution occurred within the hydrothermal system at decreasing temperature, from earlier, higher-salinity to later, low-salinity aqueous fluids. This kind of fluid evolution closely matches that of many magmatic-hydrothermal systems (e.g., BEANE and BODNAR, 1995; HEDENQUIST, 1995; GIGGENBACH, 1997). It is also in agreement with preliminary unpublished data on fluid inclusions from other tourmaline-quartz hydrothermal veins occurring in the Sesia rocks of Sessera valley, that are also close to the VDC intrusion (DIAMOND and ROSSETTI, 2000, in preparation).

During early hydrothermal stages and in the deeper portions of the VDC system, fluids must have been boron-rich, as shown by the abundance of tourmaline (SLACK, 1996). Further constrains on the pH of fluids are given by both vein and wallrock alteration assemblages. In particular, the absence of strongly acidic fluids is suggested by the absence of kaolinite and/or pyrophyllite and marcasite (MEYER and HEMLEY, 1967). A relatively high pH value during the early hydrothermal evolution is suggested by the occurrence of K-feldspar in Type I veins and associated wallrock alteration assemblage, while a progressively de-

crease in pH is documented by the occurrence of sericite ± K-feldspar and sericite only, in the alteration associated with Type II and Type III veins, respectively (ROSE and BURT, 1979; HENLEY, 1984). A similar pH decrease, from near-neutral to slightly acidic conditions, is also commonly reported in magmatic-hydrothermal systems and is probably due to cooling only (GIGGENBACH, 1997). A reducing character of the fluids is suggested by the very low Fe^{3+}/Fe_{tot} ratio calculated for tourmaline and by the local occurrence of graphite in the alteration assemblage of Type II veins. LogfS_2 values around –5 to –10 are indicated by the composition of arsenopyrite in equilibrium with pyrite in Type II veins.

6. Conclusions

The tourmaline-rich, ore-bearing veins and breccia pipes of the lower VDC represent a late-Alpine boron-rich hydrothermal system related to Oligocene magmatism in the western Alps. The emplacement of the VDC Pluton at a shallow crustal level constrains the bottom of hydrothermal system (Scaluggia area) to about 2 km below the then-existing surface, whilst the very top (Passobreve area) occurs within the andesite cover of the Sesia Zone.

The hydrothermal system shows a strong zonation in fabric, occurrence and composition of mineral assemblages from deeper to shallower levels. In the portions closer to the VDC Pluton, the system is characterized by both veins and breccia pipes, and is strongly enriched in tourmaline. Apart from pyrite and chalcopyrite, this area is relatively depleted in ore minerals. In the upper part of the system, breccia pipes do not occur, and hydrothermal veins are strongly enriched in ore minerals. In the andesite volcanics tourmaline only occurs as an accessory phase. Such vertical zoning may be related to a decrease in temperature in both space and time, as suggested by arsenopyrite and chlorite geothermometry and by fluid inclusion petrography. The occurrence of Ag, Bi and Te minerals in the upper parts of the system is also in agreement (GUILBERT and PARK, 1986; STONE and EXLEY, 1986) with a shallower and cooler environment at Passobreve.

The abundance of tourmaline, particularly in the deeper part of the system, may be ascribed to interaction between magmatic, boron-rich fluids and Al-rich wallrocks. A major role of the magmatic fluids is also suggested by the occurrence of breccia pipes in the Scaluggia area. Similar breccia bodies are typically reported in association with shallow intrusives (particularly in porphyry-like systems), and are generally interpreted as result of the escape of overpressurized fluids from the volatile-saturated upper part of shallow-level solidifying intrusions (BURNHAM, 1979; HEDENQUIST, 1995). Multistage brecciation observed in the breccia pipes may be due to repeated episodes of fluid overpressure, fluid escape and sealing of the hydrothermal conduits, according to BURNHAM's (1979, 1997) models.

The change of both fluid composition and mineral assemblages in the shallower parts of the system concomitant with a T decrease (particularly during later stages) may be due to different processes. These include interaction of fluid(s) with different wallrock types and, possibly, the increasing importance of meteoric fluids, as suggested by the occurrence of late aqueous fluid inclusions, and frequently documented in the upper parts of magmatic-related hydrothermal systems (DILLES and EINAUDI, 1992; ZALUSKI et al., 1994). At least within the andesite volcanics, brittle tectonic, related to the nearby Insubric Line, may also have played a role in the (re-)mobilization of vein material. Further studies, including radiogenic or stable isotope and absolute age determinations, are needed in order to resolve these open questions.

Acknowledgements

The authors are grateful to Ezio Callegari, Larryn Diamond and Oleg Medeot for fruitful discussions at several steps of this work. John L. Walshe's comments and calculations with his chlorite geothermometer were greatly appreciated. We thank Paolo Garofalo for discussing some petrologic aspects of fluid-mineral equilibria. Jeanne Griffin kindly reviewed the English. We gratefully acknowledge comments by Martin Engi and constructive reviews by two anonymous referees that helped to clarify and improve the manuscript. Financial support was provided by a University of Torino grant (to Roberto Compagnoni).

References

AFIFI, A.M. and ESSENE, E.J. (1988): Minfile: a microcomputer program for storage and manipulation of chemical data on minerals. Amer. Mineralogist, 73, 446–447.

ALLMAN-WARD, P., HALLS, C., RANKIN, A. and BRISTOW, C.M. (1982): An intrusive hydrothermal breccia body at Wheal Remfry in the western part of the St. Austell granite pluton, Cornwall, England. In: EVANS, A.M. (ed): Metallization associated with acid magmatism. John Wiley and Sons, New York, 1–28.

AQUATER (1992): L'oro nelle Alpi Occidentali. Ricerca Mineraria di Base, Direzione Generale delle Miniere. Ministero dell'Industria, del Commercio e dell'Artigianato, Roma.

AQUATER (1994): Ricerca di base per Mo - W (Cu - Au) nell'area indiziata della Valle del Cervo. Ricerca Mineraria di Base, Direzione Generale delle Mi-

niere. Ministero dell'Industria, del Commercio e dell'Artigianato, Roma.

BAKER, E.M. and ANDREWS, A.S. (1991): Geologic, fluid inclusion, and stable isotope studies of the gold-bearing breccia pipe at Kidston, Queensland, Australia. Economic Geology, 86, 810–830.

BEANE, R.E. and BODNAR, R.J. (1995): Hydrothermal fluids and hydrothermal alteration in porphyry copper deposits. In: PIERCE, F.W. and BOHM, J.G. (eds): Porphyry Copper Deposits of the American Cordillera. Arizona Geol. Soc. Digest, 20, 83–93.

BECCALUVA, L., BIGIOGGERO, B., CHIESA, S., COLOMBO, A., FANTI, G., GATTO, G.O., GREGNANIN, A., MONTRASIO, A., PICCIRILLO, E.M. and TUNESI, A. (1983): Post collisional orogenic dyke magmatism in the Alps. Mem. Soc. Geol. It., 26, 341–359.

BERNARDELLI, P. (1998): Studio geologico, petrografico e giacimentologico delle tormaliniti idrotermali della Valle del Cervo (Biella). Unpubl. Diploma Thesis, University of Torino, 304 pp.

BIANCHI, A. and DAL PIAZ, G.B. (1963): Gli inclusi di "micascisti eclogitici" della Zona Sesia nella formazione porfiritica permiana della Zona del Canavese fra Biella e Oropa. Giornale di Geologia, 31, 39–76.

BIGI, G., CASTELLARIN, A., COLI, M., DAL PIAZ, G.V., SARTORI, R., SCANDONE, P. and VAI, G.B. (eds) (1990): Structural Model of Italy, Sheet 1. C.N.R., S.E.L.C.A., Florence, Italy.

BIGIOGGERO, B., COLOMBO, A., DEL MORO, A., SACCHI, R. and VILLA, I. (1983): Dati isotopici e radiometrici di filoni del Biellese. Convegno "Il magmatismo tardo alpino nelle Alpi", Abstract volume, Padova.

BIGIOGGERO, B., COLOMBO, A., DEL MORO, A., GREGNANIN, A., MACERA, P. and TUNESI, A. (1994): The Oligocene Valle Cervo Pluton: an example of shoshonitic magmatism in the Western Italian Alps. Mem. Soc. Geol. It., 46, 409–421.

BIINO, G. and COMPAGNONI, R. (1989): The Canavese Zone between the Serra d'Ivrea and the Dora Baltea river (Western Alps). Eclogae geol. Helv., 82, 413–427.

BURNHAM, C.W. (1979): Magmas and hydrothermal fluids. In: BARNES, H.L. (ed): Geochemistry of hydrothermal ore deposits, 2nd Ed. John Wiley and Sons, New York, 71–133.

BURNHAM, C.W. (1997): Magmas and hydrothermal fluids. In: BARNES, H.L. (ed): Geochemistry of hydrothermal ore deposits, 3rd Ed. John Wiley and Sons, New York, 63–124.

BURT, D.M. (1989): Vector representation of tourmaline composition. Amer. Mineralogist, 74, 826–839.

CARRARO, F. (1962): Principali risultati della campagna di rilevamento 1961–62 nell'area del F.° 43 (Biella) della Carta Geologica d'Italia. Boll. Serv. Geol. It., 83, 61–69.

CARRARO, F. and FERRARA, G. (1968): Alpine "tonalite" at Miagliano, Biella (Zona dioritico-kinzigitica): a preliminary note. Schweiz. Mineral. Petrogr. Mitt., 48, 75–80.

CASTELLI, D., CONNOLLY, J.A.D. and FRANCESCHI, G. (1997): VERTEXVIEW: an interactive program to analyze and plot petrological phase diagrams. Computers and Geosciences, 23, 883–887.

CHAROY, B. (1982): Tourmalinization in Cornwall, England. In: EVANS, A.M. (ed): Mineralization Associated with Acid Magmatism. John Wiley and Sons, New York, 63–70.

CHATELINEAU, M.C. (1988): Cation site occupancy in chlorites and illites as a function of temperature. Clay Miner., 23, 471–485.

CHATELINEAU, M.C. and NIEVA, D. (1985): A chlorite solid solution geothermometer. The Los Azufres (Mexico) geothermal system. Contrib. Mineral. Petrol., 91, 235–244.

COMPAGNONI, R., DAL PIAZ, G.V., HUNZIKER, J.C., GOSSO, G., LOMBARDO, B. and WILLIAMS, P.F. (1977): The Sesia-Lanzo Zone, a slice of continental crust with alpine high pressure - low temperature assemblages in the Western Italian Alps. Rend. Soc. It. Mineral. Petrol., 33, 281–334.

CONNOLLY, J.A.D. (1990): Multivariable phase diagrams: an algorithm based on generalized thermodynamics. Amer. J. Sci., 290, 666–718.

CONNOLLY, J.A.D., MEMMI, I., TROMMSDORFF, V., FRANCESCHELLI, M. and RICCI, C.A. (1994): Forward modeling of calc-silicate microinclusions and fluid evolution in a graphitic metapelite, northeast Sardinia. Amer. Mineralogist, 79, 960–972.

DE CARITAT, P., HUTCHEON, I. and WALSHE, J.L. (1993): Chlorite geothermometry: a review. Clay Miner., 41, 219–239.

DEER, W.A., HOWIE, R.A. and ZUSSMAN, J. (1986): Rock-forming Minerals. Volume 1B: Disilicates and Ring Silicates. Longman Scientific and Technical, 629 pp.

DILLES, J.H. and EINAUDI, M.T. (1992): Wall-rock alteration and hydrothermal flow paths about the Ann-Mason porphyry copper deposit, Nevada – A 6-km vertical reconstruction. Economic Geology, 87, 1963–2001.

DROOP, G.T.R., LOMBARDO, B. and POGNANTE, U. (1990): Formation and distribution of eclogite facies rocks in the Alps. In: CARSWELL, D.A. (ed): Eclogite facies rocks. Blackie and Son, London, 225–259.

FIORENTINI POTENZA, M. (1959): Distribuzione delle principali facies petrografiche e della radioattività nel plutone "sienitico" di Biella (Valle del Cervo). Rend. Soc. It. Mineral. Petrol., 15, 89–131.

FORNASERO, D. (1978): Studio geologico-petrografico dell'aureola termometamorfica del plutone della Valle del Cervo (Biella). Unpubl. Diploma Thesis, University of Torino, 186 pp.

GAROFALO, P., AUDÉTAT, A., GÜNTHER, D., HEINRICH, C.A. and RIDLEY, J. (2000): Estimation and testing of standard molar thermodynamic properties of tourmaline end-members using data of natural samples. Amer. Mineralogist, 85, 78–88.

GIGGENBACH, W.F. (1997): The origin and evolution of fluids in the magmatic-hydrothermal system. In: BARNES, H.L. (ed): Geochemistry of hydrothermal ore deposits, 3rd Ed. John Wiley and Sons, New York, 737–796.

GUILBERT, J.M. and PARK, C.F. (1986): The geology of ore deposits. Freeman and Co., New York, 985 pp.

HAWTHORNE, F.C. (1996): Structural mechanism for light-element variations in tourmaline. Canad. Mineralogist, 34, 123–132.

HAWTHORNE, F.C. and HENRY, D.J. (1999): Classification of the minerals of the tourmaline group. Eur. J. Mineral., 11, 201–215.

HEDENQUIST, J.W. (1995): The ascent of magmatic fluids: discharge versus mineralization. In: THOMPSON, J.F.H. (ed): Magmas, Fluids, and Ore Deposits. MAC Short Course Series, 23, 263–289.

HENLEY, R.W. (1984): pH calculations for hydrothermal fluids. In: ROBERTSON, J.M. (ed): Fluid-Mineral Equilibria in Hydrothermal Systems. Reviews in Economic Geology, 1, 83–98.

HENRY, D.J. and DUTROW, B.L. (1996): Metamorphic tourmaline and its petrologic applications. In: GREW, E.S. and ANOVITZ, L.M. (eds): Boron: mineralogy,

petrology and geochemistry. MSA Reviews in Mineralogy, 33, 503–557.

HENRY, D.J. and GUIDOTTI, C.V. (1985): Tourmaline as a petrogenetic indicator mineral: an example for staurolite-grade metapelite of NW Maine. Amer. Mineralogist, 70, 1–15.

HEY, M. H. (1954): A new review of the chlorites. Mineral. Mag., 30, 277–292.

HOLLAND, T.J.B. and POWELL, R. (1998): An internally consistent thermodynamic data set for phases of petrological interest. J. Metamorphic Geol., 16, 309–344.

HUNZIKER, J.C. (1974): Rb/Sr and K/Ar age determinations and the Alpine tectonic history of the Western Alps. Mem. Ist. Geol. Min. Univ. Padova, 31, 55 pp.

JACKSON, N.J., HALLIDAY, A.N., SHEPPARD, S.M.F. and MITCHELL, J.G. (1982): Hydrothermal activity in the St Just mining district, Cornwall, England. In: Evans, A.M. (ed.): Metallization Associated with Acid Magmatism. John Wiley and Sons, New York, 137–179.

JACKSON, N.J., WILLIS-RICHARDS, J., MANNING, D.A.C. and SAMS, M.S. (1989): Evolution of the Cornubian ore field, southwest England: part II. Mineral deposits and ore-forming processes. Economic Geology, 84, 1101–1133.

JIANG, S.Y., PALMER, M.R., LI, Y.H. and XUE, C.Y. (1995): Chemical composition of tourmaline in the Yindongzi-Tongmugou Pb–Zn deposits, Qinling, China: implications for hydrothermal ore-forming processes. Mineralium Deposita, 30, 225–234.

JOWETT, E.C. (1991): Fitting iron and magnesium into the hydrothermal chlorite geothermometer. GAC/MAC/SEG Joint Annual Meeting, Toronto, Program with Abstracts, 16, A62.

KERESTEDJIAN, T. (1997): Chemical and morphological features of arsenopyrite, concerning its use as a geothermometer. Mineralogy and Petrology, 60, 231–243.

KNOPF, A. (1913): The tourmalinitic silver-lead type of ore deposits. Economic Geology, 8, 105–119.

KRETSCHMAR, U. and SCOTT, S.D. (1976): Phase relations involving arsenopyrite in the system Fe–As–S and their application. Canad. Mineralogist, 14, 364–386.

KRETZ, R. (1973): Symbols for rock-forming minerals. Amer. Mineralogist, 68, 277–279.

LANZA, R. (1977): Palaeomagnetic Data from the Andesitic and Lamprophyric Dikes of the Sesia-Lanzo Zone (Western Alps). Schweiz. Mineral. Petrogr. Mitt., 57, 281–290.

LANZA, R. (1979): Palaeomagnetic data on the andesitic cover of the Sesia-Lanzo Zone (Western Alps). Geol. Rundsch., 68, 83–92.

LANZA, R. (1984): Palaeomagnetism in the Traversella Massif. Boll. Geofis. Teor. Appl., 26, 115–124.

LONDON, D. and MANNING, D.A.C. (1995): Chemical variation and significance of tourmaline from Southwest England. Economic Geology, 90, 495–519.

LONDON, D., HERVIG, R.L. and MORGAN, G.B. VI (1988): Melt-vapor solubilities and element partitioning in peraluminous granite-pegmatite systems: Experimental results with Macusani glass at 200 MPa. Contrib. Mineral. Petrol., 99, 360–373.

LONDON, D., MORGAN, G.B. VI and WOLF, M.B. (1996): Boron in granitic rock and their contact aureoles. In: GREW, E.S. and ANOVITZ, L.M. (eds): Boron: mineralogy, petrology and geochemistry. MSA Reviews in Mineralogy, 33, 299–329.

LYNCH, G. and ORTEGA, J. (1997): Hydrothermal alteration and tourmaline–albite equilibria at the Cox-heath Porphyry Cu–Mo–Au Deposit, Nova Scotia. Canad. Mineralogist, 35, 79–94.

MEDEOT, O. (1998): Petrologia delle vulcaniti terziarie di copertura della Zona Sesia (Alpi occidentali interne). Ph.D. Thesis, University of Torino, 130 pp.

MEDEOT, O., CALLEGARI, E. and CIGOLINI, C. (1997): Petrochemical aspects of calc-alkalic and shoshonitic post-collisional Oligocene volcanics of the cover series of the Sesia-Lanzo Zone, Western Italian Alps. Quaderni di Geodinamica Alpina e Quaternaria, 4, 77–78.

MEYER, C. and HEMLEY, J.J. (1967): Wall rock alteration. In: BARNES, H.L. (ed): Geochemistry of Hydrothermal Ore Deposits. Holt, Rinehart and Winston, New York, 166–235.

PICHAVANT, M. (1981): An experimental study on the effect of boron on a water-saturated haplogranite at 1 kbar vapour pressure: geological applications. Contrib. Mineral. Petrol., 76, 430–439.

RIMIN (1989): Potenziale metallogenico delle plutoniti post-erciniche dell'arco Alpino. Ricerca Mineraria di Base, Direzione Generale delle Miniere. Ministero dell'Industria, del Commercio e dell'Artigianato, Roma.

ROMER, R.L., SCHÄRER, U. and STECK, A. (1996): Alpine and pre-Alpine magmatism in the root-zone of the western Central Alps. Contrib. Mineral. Petrol., 123, 138–158.

ROSE, A.W. and BURT, D.M. (1979): Hydrothermal alteration. In: BARNES, H.L. (ed): Geochemistry of Hydrothermal Ore Deposits, 2nd Ed. John Wiley and Sons, New York, 173–235.

SCHEURING, B., AHRENDT, H., HUNZIKER, J.C. and ZINGG, A. (1974): Palaeobotanical and geochronological evidence for the Alpine Age of the metamorphism in the Sesia-Zone. Geol. Rundsch., 63, 305–326.

SHARP, Z.D., ESSENE, E.J. and KELLY, W.C. (1985): A re-examination of the arsenopyrite geothermometer: pressure consideration and applications to natural assemblages. Canad. Mineralogist, 23, 517–534.

SHELNUTT, J.P. and NOBLE, D.C. (1985): Premineralization radial dikes of tourmalinized fluidization breccia, Julcani District, Peru. Economic Geology, 80, 1622–1632.

SILLITOE, R.H. (1985): Ore-related breccias in vulcanoplutonic arc. Economic Geology, 80, 1467–1514.

SILLITOE, R.H. and SAWKINS, F.J. (1971): Geologic, mineralogic and fluid inclusion studies relating to the origin of copper-bearing tourmaline breccia pipes, Chile. Economic Geology, 66, 1028–1041.

SLACK, J.F. (1996): Tourmaline associations with hydrothermal ore deposits. In: GREW, E.S. and ANOVITZ, L.M. (eds): Boron: mineralogy, petrology and geochemistry. MSA Reviews in Mineralogy, 33, 559–643.

STONE, M. and EXLEY, B. (1986): High heat production granites of southwest England and their associated mineralization: a review. Trans. Instn. Min. Metall. (Sect. B: Appl. Earth Sci.), 95, B25–36.

TREVISIOL, M. (1999): Studio geologico petrologico del nucleo "granitico" del plutone della Valle Cervo. Unpubl. Diploma Thesis, University of Torino, 121 pp.

ULMER, P. (1993): Norm-program for cation and oxygen mineral norms. Computer Library IKP-ETH, Zürich.

VENTURELLI, G., THORPE, R.S., DAL PIAZ, G.V., DEL MORO, A. and POTTS, P.J. (1984): Petrogenesis of calc-alkaline, shoshonitic and associated ultrapotassic Oligocene volcanic rocks from the Northwestern Alps, Italy. Contrib. Mineral. Petrol., 86, 209–220.

WALSHE, J.L. (1986): A six-component chlorite solid solution model and the conditions of chlorite formation in hydrothermal and geothermal systems. Economic Geology, 81, 681–703.

WARNAARS, F.W. (1983): Copper tourmaline breccias at Los Bronces, Chile. Soc. Min. Engineers AIME Trans., 272, 1902–1911.

WARNAARS, F.W., HOLMGRED, C.D. and BARASSI, S.F. (1985): Porphyry copper and tourmaline breccias at Los Bronces-Rio Blanco, Chile. Economic Geology, 80, 1544–1565.

ZALUSKI, G., NESBITT, B. and MUEHLENBACHS, K. (1994): Hydrothermal alteration and stable isotope systematics of the Babine porphyry Cu deposits, British Columbia: implications for fluid evolution of porphyry systems. Economic Geology, 89, 1518–1541.

ZINGG, A., HUNZIKER, J.C., FREY, M. and AHRENDT, H. (1976): Age and degree of metamorphism of the Canavese Zone and of the sedimentary cover of the Sesia Zone. Schweiz. Mineral. Petrogr. Mitt., 56, 361–375.

Manuscript received August 17, 1999; revision accepted September 4, 2000.